

**THE RADIATION-INDUCED DEGRADATION
OF POLY(DIENE SULFONES) AS X-RAY RESISTS**

A Thesis

Submitted to the Graduate Faculty of the
Louisiana State University and
Agricultural and Mechanical College
in partial fulfillment of the
requirements for the degree of
Master of Science

in

The Department of Chemistry

by
Gina Calderon
B.S., Louisiana State University, 1995
May 2002

TABLE OF CONTENTS

ACKNOWLEDGEMENTS.....	iii
LIST OF TABLES.....	iv
LIST OF FIGURES.....	v
ABSTRACT.....	vii
CHAPTER 1. INTRODUCTION.....	1
1.1 Polysulfones in the microelectronics industry.....	1
1.1.1 The role of polymer resists.....	1
1.1.2 Polysulfones as resists.....	2
1.2 The radiation chemistry of resists.....	5
1.2.1 Absorption of radiation.....	6
1.2.2 Radiation chemical processes.....	7
1.3 Background and goals of thesis.....	11
CHAPTER 2. SPECTROSCOPIC ANALYSES OF THE RADIATION-INDUCED DEGRADATION OF POLY(OLEFIN SULFONES).....	15
2.1 X-ray Absorption Near-Edge Structure (XANES) Spectroscopy.....	15
2.1.1 Introduction.....	15
2.1.2 Measurement of x-ray absorption.....	17
2.1.3 Experimental.....	18
2.2 In situ mass spectrometry of irradiated poly(olefin sulfones).....	24
2.2.1 Introduction.....	24
2.2.2 Experimental.....	28
2.3 Discussion of spectroscopic results.....	30
2.3.1 Poly(butene sulfone) and poly(2-methyl pentene sulfone).....	31
2.3.2 Poly(3-methyl pentene sulfone) and poly(hexadiene sulfone).....	38
CHAPTER 3. SYNTHESIS OF POLY(PENTADIENE SULFONE) AND POLY(HEPTADIENE SULFONE).....	40
3.1 Introduction.....	40
3.2 Synthesis of poly(pentadiene sulfone).....	41
3.3 Synthesis of poly(heptadiene sulfone).....	43
3.3.1 Monomer synthesis – The Wittig reaction.....	43
3.3.2 Polymerization.....	48
CHAPTER 4. CONCLUSIONS.....	50
REFERENCES.....	52
VITA.....	54

ACKNOWLEDGEMENTS

First and foremost, I would like to thank my major professor Dr. William Daly for his guidance, support and patience throughout my graduate studies. For fostering my interest in microlithography and confidence in myself, I thank my former supervisor at CAMD, Olga Vladimirsky, who is also my friend and mentor. Equally supportive and important, I must also acknowledge Dr. Yuli Vladimirsky, who has encouraged me to think on a different level in all aspects. For beginning our interest in poly(olefin sulfones) as resists, I would like to acknowledge Dr. Jack Davies, who synthesized and developed the poly(olefin sulfones) as part of his PhD dissertation at LSU. For his help, support and encouragement in pursuing graduate studies, I thank Dr. Paul Schilling, who initiated the spectroscopic studies on polysulfones and gave me the instruction I needed to understand its concepts. I would also like to thank Dr. Roland Tittsworth and Dr. Eizi Morikawa at CAMD for their help and support with XANES and mass spectrometry.

In addition, I would like to thank my friends for supporting me through the bad times and laughing with me through the good. Finally, I thank my fiancée and best friend, Barry Wilkinson, for being there and believing in me. This work is dedicated to my late great-aunt, Basilisa Siruno, who raised me as her own and whose memory lives with each of my accomplishments.

LIST OF TABLES

1.1	Generation and decay of reactive intermediates.....	9
2.1	List of mass peaks and their corresponding molecular ions.....	35

LIST OF FIGURES

1.1	Chemical structures of PMMA and PBS.....	3
1.2	Chemical structures of novolac and PMPS.....	5
1.3	Initial reactions in the absorption of high-energy radiation.....	7
1.4	Decomposition pathway of PBS via a radical cation.....	10
1.5	Mechanism of radiation-induced chain scission in PMMA.....	11
1.6	Poly(diene sulfones) to be studied spectroscopically.....	13
1.7	Chemical structures of poly(pentadiene sulfone), poly(hexadiene sulfone) and poly(heptadiene sulfone).....	14
2.1	X-ray absorption spectrum showing the sulfur K-edge XANES of PBS.....	16
2.2	Sulfur K-edge XANES of reference compounds.....	20
2.3	XANES results of poly(olefin sulfones).....	21
2.4	XANES results of poly(unsaturated olefin sulfones).....	22
2.5	UV degradation products of PMMA detected with in situ mass spectrometry.....	27
2.6	Radiation degradation mechanism of poly(lactide).....	27
2.7	Experimental set-up of the mass spectrometer.....	29
2.8	Mass spectrometry results of poly(olefin sulfones).....	32
2.9	Mass spectrometry results of poly(unsaturated olefin sulfones).....	33
2.10	Mass spectrometry results for poly(cyclic aliphatic or aromatic sulfones).....	34
2.11	Decomposition pathway of PBS.....	37
2.12	Sulfur K-Edge XANES of PHS and PBS at increasing doses.....	39
3.1	1,2 addition polymerization.....	41
3.2	Copolymerization of 1,3 dienes with SO ₂	41

3.3	IR spectrum of poly(pentadiene sulfone), PPS.....	43
3.4	The Wittig reaction.....	44
3.5	Salt formation for the Wittig reaction.....	45
3.6	The Wittig reaction to form 1,3-heptadiene monomer.....	46
3.7	H ¹ NMR spectrum of synthesized 1,3-heptadiene.....	47

ABSTRACT

The microlithographic process, essential in the fabrication of silicon chip integrated circuits, uses high-energy radiation to transfer a pattern onto a thin film of polymer resist. Pattern transfer occurs by modifying the properties (solubility or volatility) of the polymer film exposed to radiation. Poly(olefin sulfones) exhibit a high sensitivity to x-rays, which is a desirable property for polymer resists, but typically undergo a glass transition around room temperature and a thermal degradation at moderate temperatures. The thermal properties of the poly(olefin sulfones) reduce the processing latitude for industrial microelectronics applications.

Poly(unsaturated olefin sulfones) containing a carbon-carbon double bond in the polymer backbone exhibit good thermal stability and film forming properties comparable to those observed with poly(methyl methacrylate), PMMA. The potential utility of these new resins prompted a study of the mechanism of degradation promoted by x-ray radiation. In this study, the effect of x-ray radiation on polysulfones with varied chemical structures was analyzed using x-ray absorption near-edge structure (XANES) spectroscopy. The volatile by-products formed upon irradiation of each polysulfone were characterized by in-situ mass spectroscopy.

Distinct differences between the mode of degradation of poly(olefin sulfones) such as poly(butane-1 sulfone), PBS, and that of poly(hexadiene sulfone), PHS, were observed. The energy positions of the sulfur K-edge in irradiated PBS are approximately 2473 eV, (sulfide) and 2479 eV (sulfone). Decomposition is accompanied by sulfide formation and the evolution of butene-1 in the gaseous by-products. In contrast, the sulfur K edge spectra of PHS exhibits the following energy positions, 2473 eV (sulfide), 2475 eV (sulfoxide), 2478 eV (sulfone) and 2482 eV (sulfonate). Only sulfur oxide by-products were observed in the mass spectra indicating that

the predominant mode of degradation is oxidative. Further studies will be required to elucidate the mechanism of this new mode of degradation.

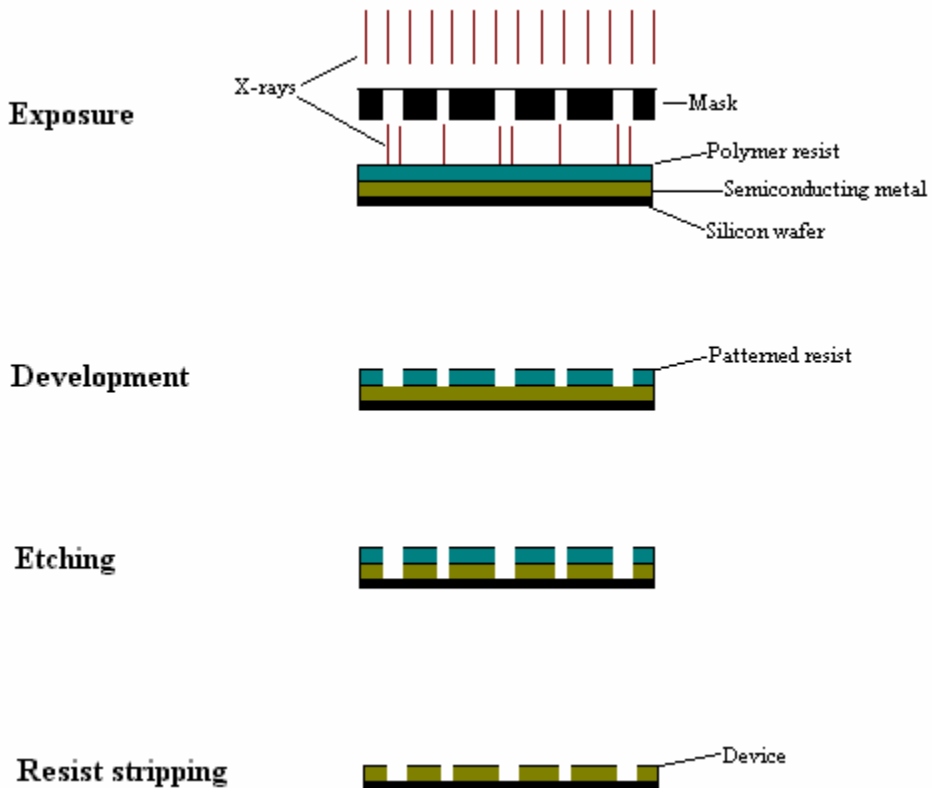
CHAPTER 1

INTRODUCTION

1.1 Polysulfones in the microelectronics industry

1.1.1 The role of polymer resists

Microlithography, an essential process in the fabrication of silicon chip integrated circuits, involves the modification of the solubility or volatility of thin polymer resist films by radiation. The lithographic process uses a mask to create a pattern in a thin film of polymer resist, which is developed after exposure to some type of radiation. After the pattern has been transferred to the polymer resist layer, the underlying metal is then etched to produce the device.



The leading method for producing devices with features as small as 0.25 μm is deep-UV lithography, utilizing radiation wavelengths around 250 nm. In the drive to improve the resolution and decrease the size of device features, resist systems have been developed to extend into regions of smaller wavelength such as the vacuum-UV. X-ray lithography, utilizing radiation wavelengths less than 1 nm, is a competitive alternative to the production of smaller nanofeatures. However, due to the difference in the absorption mechanisms of high-energy radiation, resists must be tailored for such energies. Extensive research has been done to quantify and understand the radiation mechanisms of x-ray resist systems. With this knowledge, the sensitivity and contrast of such resist systems can be improved. Important polymer properties to consider in designing resists include chemical composition and average atomic number, molecular weight, molecular weight distribution, density and glass transition temperature.³

1.1.2 Polysulfones as resists

Polysulfones have been known to have a high sensitivity to x-rays making them highly desirable resist materials for use in microlithography. The labile sulfur-carbon bond and low ceiling temperature (T_c) is key to the rapid degradation of these polymers in response to radiation. The sensitivity of resist materials can be compared using G-values, which quantify their response to ionizing radiation. For example, $G(s)$ is the number of chain scissions produced per 100 eV of absorbed energy and is described by the formula¹:

$$N^* = [G(s)/100]Dw$$

where, N^* = the total number of scissions produced in the sample

D = the irradiation dose in eV/gram

w = the weight of polymer in grams

The first polysulfone developed for commercial use as an e-beam resist was poly(butene-1 sulfone) (PBS), which exhibits a G(s) of 12.2. The classical x-ray resist poly(methyl methacrylate) (PMMA) exhibits a G(s) around 2.²

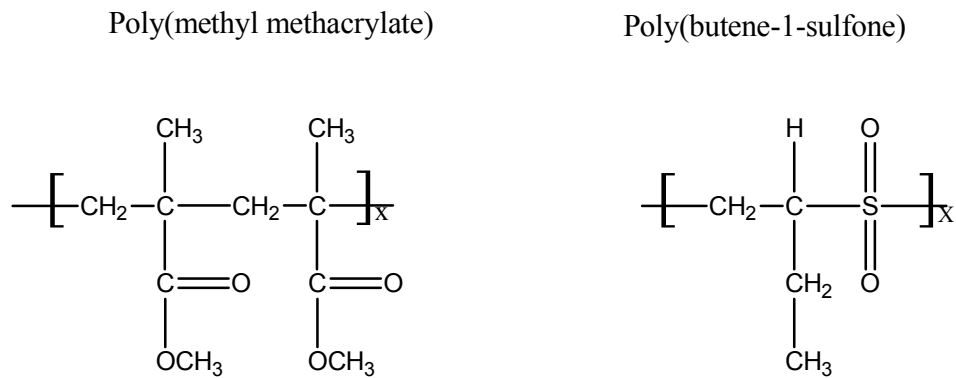


Figure 1.1 Chemical structures of PMMA and PBS

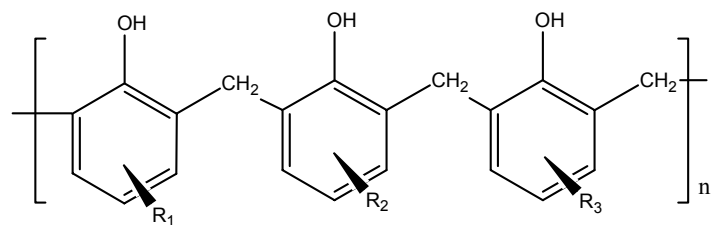
The problem with polysulfones, however, is their low thermal stability due to their low glass transition temperature and the difficulty in forming good films for lithographic processing due to limited solubility in solvents for spin-coating.³ These complications reduce the processing latitude of polysulfones for industrial microelectronics applications. However, the high sensitivity of these polymers has led to several modifications to overcome these problems.

Poly(butene-1 sulfone), developed by Bell Laboratories, is widely used as a resist for e-beam lithography. Exposure to e-beam radiation results in main-chain scission of the carbon-sulfur bond followed by a temperature dependent depolymerization of the

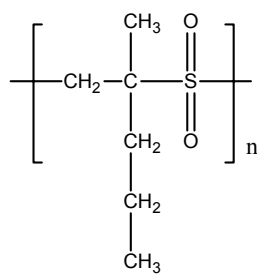
radical fragments into volatile monomer species. The rapid depolymerization of sulfone polymers contributes to their high radiation sensitivity. However, this high sensitivity limits the processing applicability of the polymer to wet chemical etching. Sulfone polymers are not only sensitive to e-beam radiation, but also to plasma and reactive ion etching environments, making them unsuitable for dry etching procedures.

In order to circumvent the problem of dry etch resistance in sulfone polymers, Bell Laboratories developed a two component resist system incorporating the polysulfone into a novolac matrix resin, commonly used in diazoquinone-novolac photoresist materials. Novolac resins have excellent film-forming characteristics and etch resistance. The polysulfone acts as a photoactive dissolution inhibitor. As an intact polymer, the polysulfone inhibits the dissolution of the novolac resin in the developer solution. Exposure to radiation degrades the polymer, removing the dissolution inhibitor and the novolac becomes more soluble in the developer solution. This design has been successfully used in several mask fabrication facilities in the US and Japan. The chemical structures of novolac and the polysulfone used in NPR, the Bell version of this system, are shown in Figure 1.2.¹

One attempt at improving the processing of polysulfones for lithographic applications involved the development of poly(diene sulfones) with inherent properties of thermal stability and film-forming characteristics comparable to PMMA. The inclusion of double bonds into the main chain and the addition of large alkyl side groups proved to be successful modifications.



Novolac Copolymer



Poly(2-methyl-1-pentene sulfone)

Figure 1.2 Chemical structures of novolac and PMPS.

1.2 The radiation chemistry of resists

Radiation chemistry is the study of the chemical effects of high energy, ionizing radiation on the properties of materials. High energy radiation includes electromagnetic radiation having kinetic energies much higher than bond dissociation energies, such as x-rays and γ -rays. X-rays are produced either by electron bombardment of a metal target, or in a synchrotron. Synchrotron radiation is emitted by high-energy electrons, which are accelerated by a magnetic field and circulate in a storage ring. The spectrum obtained by synchrotron radiation extends from the microwave into the x-ray region. Soft x-rays with wavelengths (λ) greater than 4 Angstroms (0.4 nm) are of particular interest for promoting the degradation of x-ray sensitive polymer resists.²

1.2.1 Absorption of radiation

The absorption of optical radiation ($\lambda \sim 150\text{-}1300\text{ nm}$), which includes ultraviolet, visible and infrared radiation, involves the interaction with chromophoric groups within the polymer. Chromophores are selective sites within a polymer that are capable of absorbing a given photon of energy.² Photons at wavelengths below about 250 nm have enough energy to break most of the C-C, C-H, C-Halogen, C-O, O-O, and O-H bonds in polymers.⁴ When polymer molecules are irradiated with photon energies smaller than the ionization potential, chemical changes are initiated by generating excited states.²

In contrast, the absorption of high-energy electromagnetic radiation, which includes x-rays and γ -rays, does not involve the interaction of specific chromophoric groups. Instead, absorption occurs via interactions with both the nuclei of atoms and the clouds of electrons surrounding them. However, if the incident radiation consists of photon or kinetic energies lower than about 10 MeV, and the irradiated material consists only of light nuclei such as C, O, H, N, S and P, the interactions with the atomic nuclei can be neglected. The absorption of soft x-rays by polymeric materials involves the interaction of radiation with electrons in the atomic or molecular orbitals.²

The radiation chemistry resulting from the absorption of high-energy radiation occurs mainly through the interaction of secondary electrons within the polymer molecules. Absorption can result in pair production, the photoelectric effect or Compton scattering. In the photoelectric effect, the energy of the incident photon is used to eject an electron, usually from an inner valence shell orbital of the atom. In Compton scattering part of the energy of the incident photon is used to eject an electron, and the remainder of the energy results in a secondary electron of lower energy. In either case,

secondary electrons are ejected, which possess enough kinetic energy to induce additional ionizations or electronic excitations in surrounding molecules.⁵ Figure 1.3 illustrates the initial reactions that occur in the absorption of high-energy radiation.²

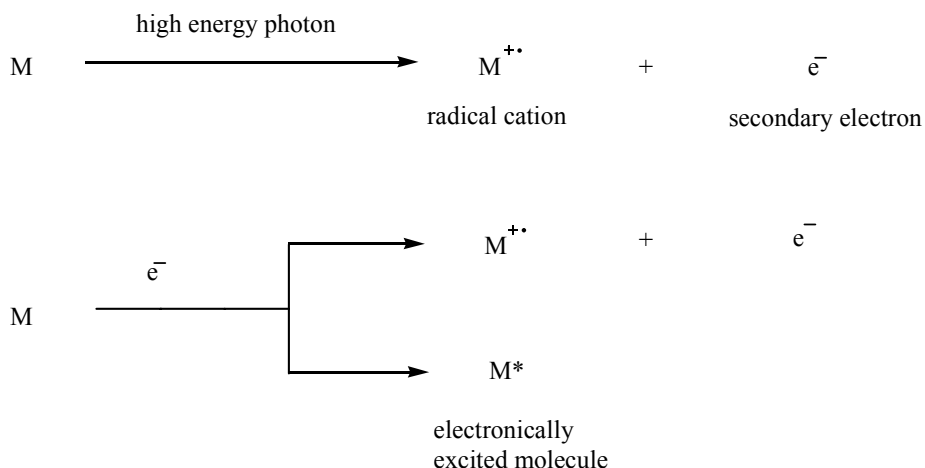


Figure 1.3 Initial reactions in the absorption of high-energy radiation.

It is generally known that resist materials that are sensitive to e-beam radiation are also sensitive to x-ray radiation and function in the same fashion. This is because of the fact that the radiation chemistry results from the interaction of secondary electrons with the resist material, and the secondary electrons produced by γ -rays, x-rays or e-beam radiation all look the same to resist molecules.⁵

1.2.2 Radiation chemical processes

The initial chemical reactants produced by the absorption of radiation in a polymer consist of various unstable and transient species such as ions, radicals and electronically excited molecules. The chemical processes that occur within a polymeric film are complicated because of the transience of the reaction intermediates, and also because processes frequently occur through several reaction routes. The various

reactions involved in generating intermediate species are given in Table 1.1.² Thus our knowledge about the mechanisms of high-energy radiation-induced degradation processes in polymers is still limited and further understanding is highly desirable. In the chemistry of positive tone resists, the resultant excited molecule may undergo bond scission. Chain scission causes a decrease in the molecular weight of the polymer, resulting in an increase in the dissolution rate of the exposed area. In some polysulfones, chain scission results in self-development where the irradiated polymer is degraded into volatile products. The mechanism of main-chain degradation of poly(methyl methacrylate), PMMA, presented in Figure 1.5, is a typical example of radiation-induced polymer chain cleavage.

The enhanced radiation sensitivity of polysulfones is attributed to the high sensitivity of the $-\text{SO}_2-$ group. For example, upon exposure to e-beam radiation poly(butene 1-sulfone), PBS, undergoes main chain scission to produce, as main products, sulfur dioxide and the olefin monomer, 1-butene. Other radiation sensitive groups include COOH , C-Hal , NH_2 and C=C . In contrast, aromatic groups are known to be resistant to radiation.⁵ The radiation-induced degradation of PBS and PMMA, are illustrated in Figures 1.4 and 1.5.¹

Primary radiolytic act	$M \longrightarrow M^{\bullet+} + e^{-}$
Capture of thermalized electron by positive ion	$M^{\bullet+} + e_{\text{th}}^{-} \longrightarrow M^*$
Capture of thermalized electron by neutral molecule	$M + e_{\text{th}}^{-} \longrightarrow M^{\bullet-}$
<i>Bond breaking reactions:</i>	
Radical formation	$M^* \longrightarrow R_1^{\bullet} + R_2^{\bullet}$
Decomposition of positive radical ion	$M^{\bullet+} \longrightarrow R^{\bullet} + A^{+}$
Decomposition of negative radical ion	$M^{\bullet-} \longrightarrow R^{\bullet} + B^{-}$
Decomposition of excited molecule	$M^* \longrightarrow C + D$
<i>Side reactions:</i>	
Charge transfer	$M^{\bullet+} + S \longrightarrow M + S^{\bullet+}$
	$M^{\bullet-} + S \longrightarrow M + S^{\bullet-}$
Energy transfer	$M^* + S \longrightarrow M + S^*$

Table 1.1 Generation and decay of reactive intermediates

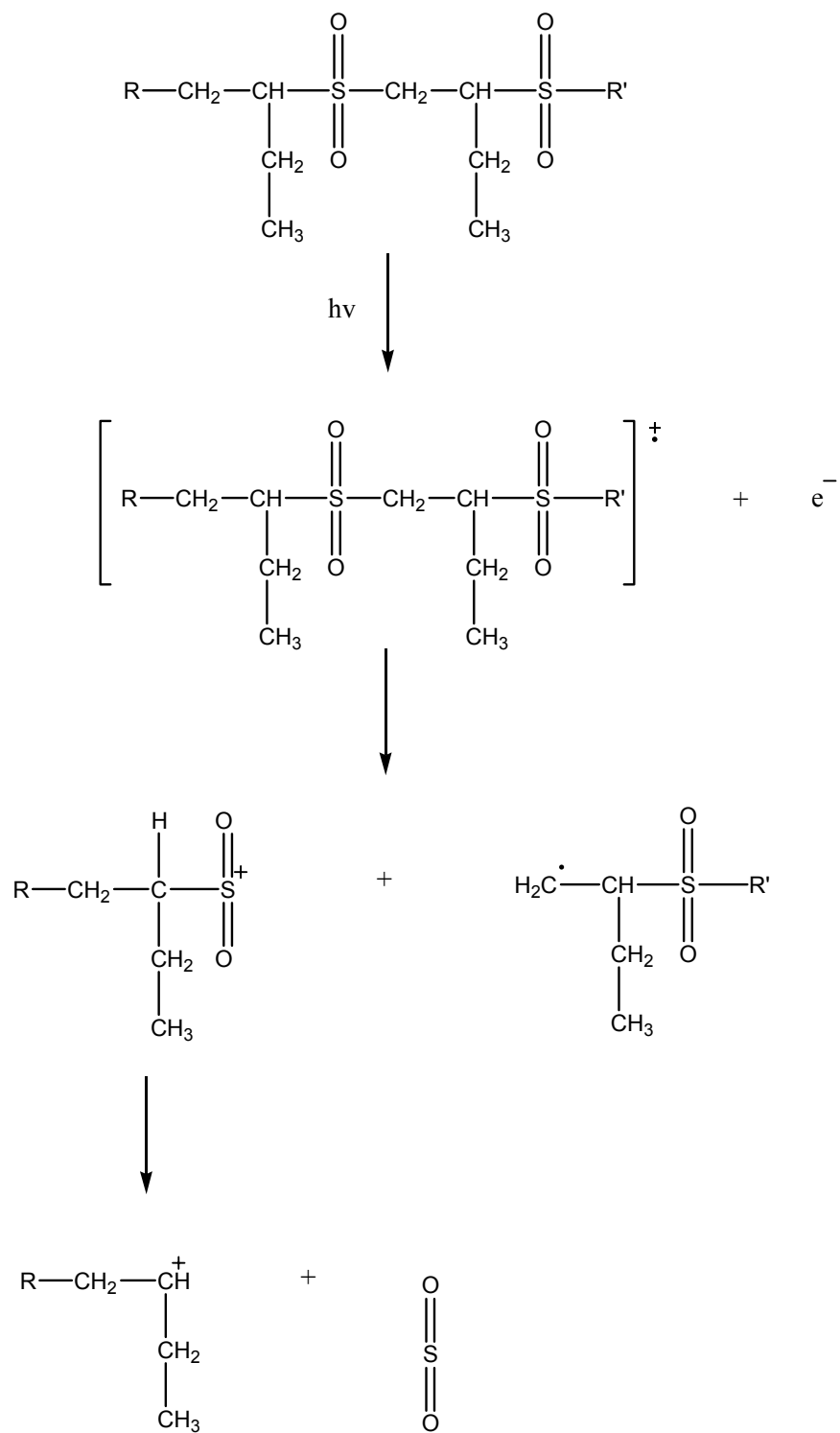


Figure 1.4 Decomposition pathway of PBS via a radical cation.

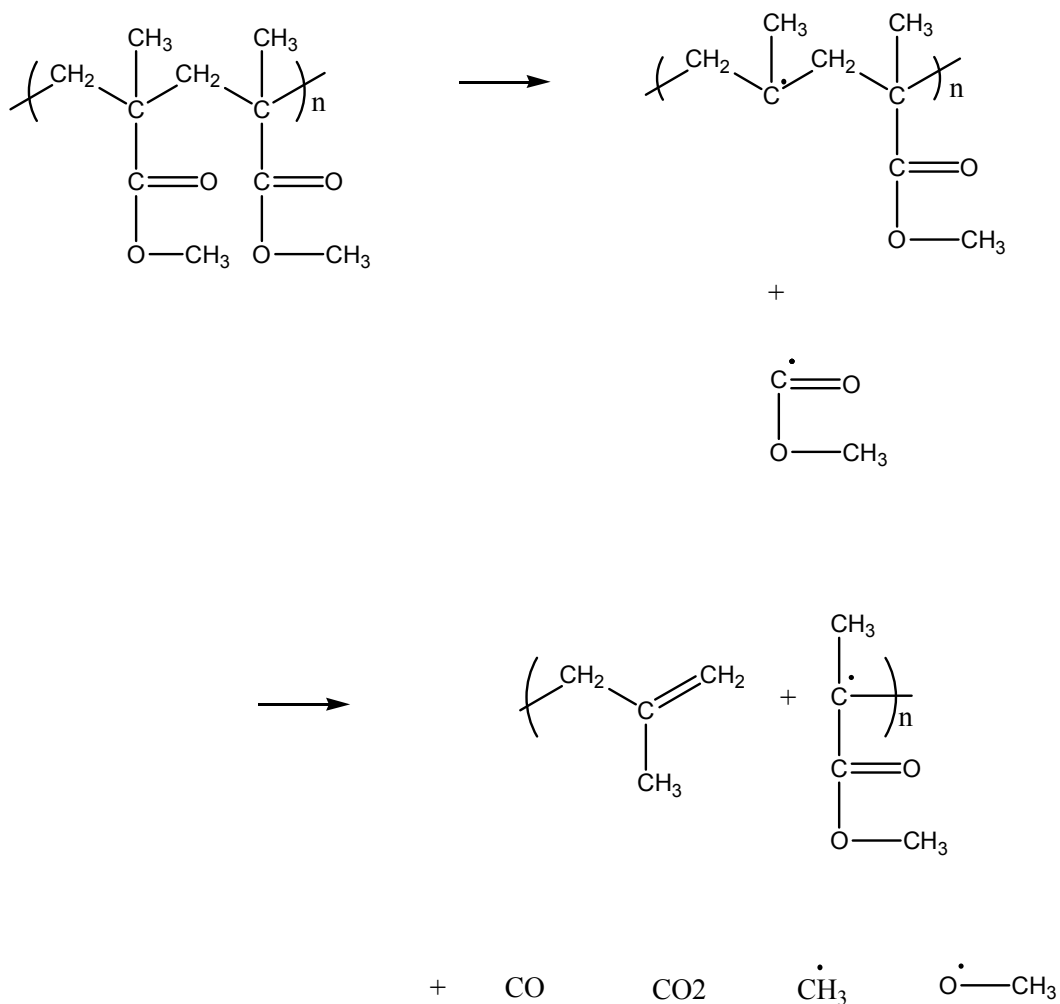


Figure 1.5 Mechanism of radiation-induced chain scission in PMMA.

1.3 Background and goals of this thesis

As part of a PhD dissertation in the Department of Chemistry at LSU, several poly(diene sulfones) were synthesized and characterized to investigate their potential as x-ray resists. It was revealed that they possess high sensitivity to x-ray radiation; however, their solubilities and respective film-forming capabilities varied. In order to increase the glass transition temperatures of the polymers, modifications were incorporated to decrease bond rotation about the main chain. For example, bulky side

groups were introduced to decrease chain mobility. In addition, a double bond was incorporated into the backbone. To increase the solubility of the polymers, larger alkyl substituents were incorporated into the side groups. Among the group of polymers studied, poly(hexadiene-1,3 sulfone), PHS, was proposed and patented as a potential x-ray resist because of its high sensitivity and good film-forming capabilities.¹⁵

In order to elucidate the chemical effect of x-ray radiation on the new polysulfone resists such as PHS, the poly(diene sulfones) were investigated spectroscopically. X-ray absorption near edge structures (XANES) spectroscopy were performed on the polysulfones both before and after irradiation to observe the changes in the sulfur atom, which is involved in the main chain scission of the polymer. In addition, in situ mass spectrometry was performed to detect gaseous species evolving from the polymers during irradiation. Spectroscopic results were compared to gain insight into their mechanisms of degradation. Figure 1.6 shows the structures of the polymers studied.

A radical addition polymerization with SO₂ was performed to synthesize two polysulfones: poly(pentadiene sulfone) or PPS, and poly(heptadiene sulfone) or PHS2. The chemical structures of the polymers are given in Figure 1.7. It is believed that the glass transition temperature and the solubility of PHS2 should be higher than that of PHS due to the longer alkyl side chain.

The ultimate goal is to postulate possible mechanisms for the radiation-induced degradation of different polysulfones, based on their chemical structures. Knowledge of such mechanisms will be a valuable asset in the design of new and improved sulfur-based polymer resist systems.

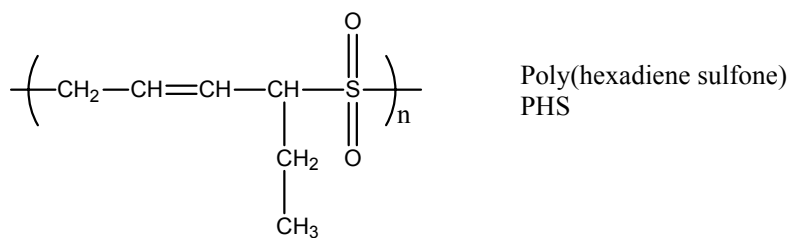
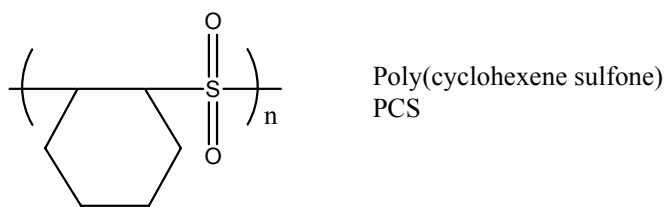
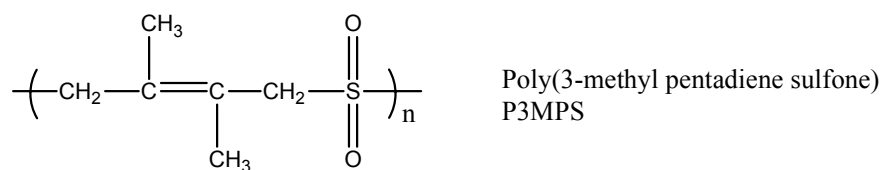
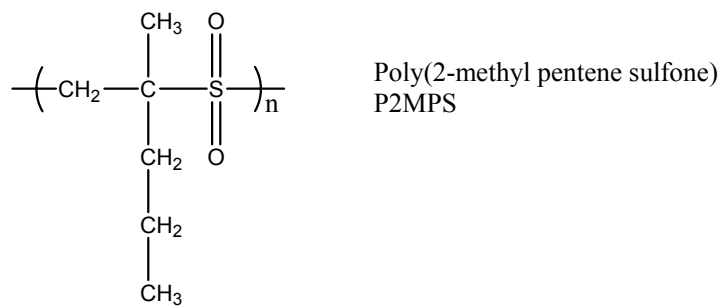
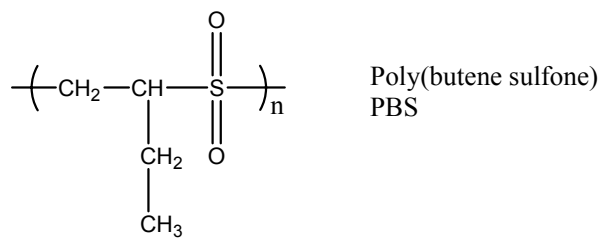
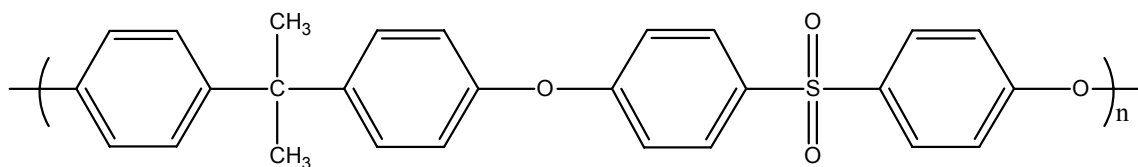
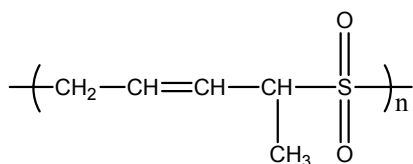


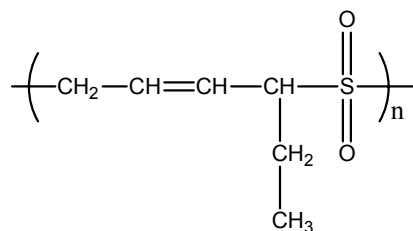
Figure 1.6 Polydiene sulfones to be studied spectroscopically. (Figure continued)



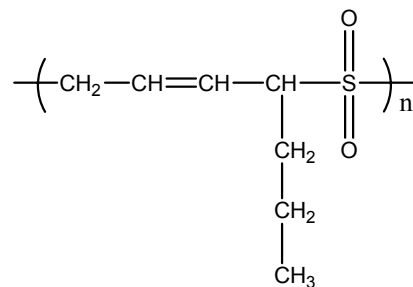
Poly(ether sulfone) resin
PSR



Poly(pentadiene sulfone)
PPS



Poly(hexadiene sulfone)
PHS



Poly(heptadiene sulfone)
PHS2

Figure 1.7 Chemical structures of poly(pentadiene sulfone), PPS; poly(hexadiene sulfone), PHS; and poly(heptadiene sulfone), PHS2.

CHAPTER 2

SPECTROSCOPIC ANALYSES OF THE RADIATION-INDUCED DEGRADATION OF POLY(OLEFIN SULFONES)

2.1 X-ray Absorption Near-Edge Structure (XANES) Spectroscopy

2.1.1 Introduction

X-ray absorption spectroscopy has been a fundamental tool in giving information on the electronic structure of atoms. The characteristic x-ray spectra of the elements allow scientists to investigate molecular systems based on the absorbing atom. For example, in XPS (X-ray Photoelectron Spectroscopy) the energy of the incident photon is great enough to eject electrons from inner cores of atoms.¹² However, this technique is not used in this study because of the insulating property of the polymers, which would broaden the signal obtained from XPS. An alternative, XANES spectroscopy, is a particularly good method for seeing the electronic changes occurring in the polymers being studied. In particular, K-edge XANES gives information corresponding to the most tightly bound core electrons in the $n=1$ shell. The L-edge corresponds to the $n=2$ shell.⁶

The x-ray absorption spectrum of an atom can be viewed as consisting of two regions: the lower energy XANES region (X-ray Absorption Near Edge Structures), and the higher energy EXAFS region (Extended X-ray Absorption Fine Structures). The x-ray absorption spectrum showing the sulfur K-edge XANES of PBS is shown in Figure 2.1.⁶

The XANES region of the absorption spectrum is divided into three areas. Generally, the XANES region of a spectrum begins at the “absorption threshold”, which corresponds

to the photon energy at which an electron in the atom reaches the lowest energy state of core excitations. Following this region is the “absorption edge”, a steep rise in the absorption coefficient of the spectrum, in which the photon energy is enough to excite an electron to the first empty electronic states, or bound states, which may be available within the atom. Finally, the “ionization threshold” is the photon energy at which the electron is ejected from the atom.⁷

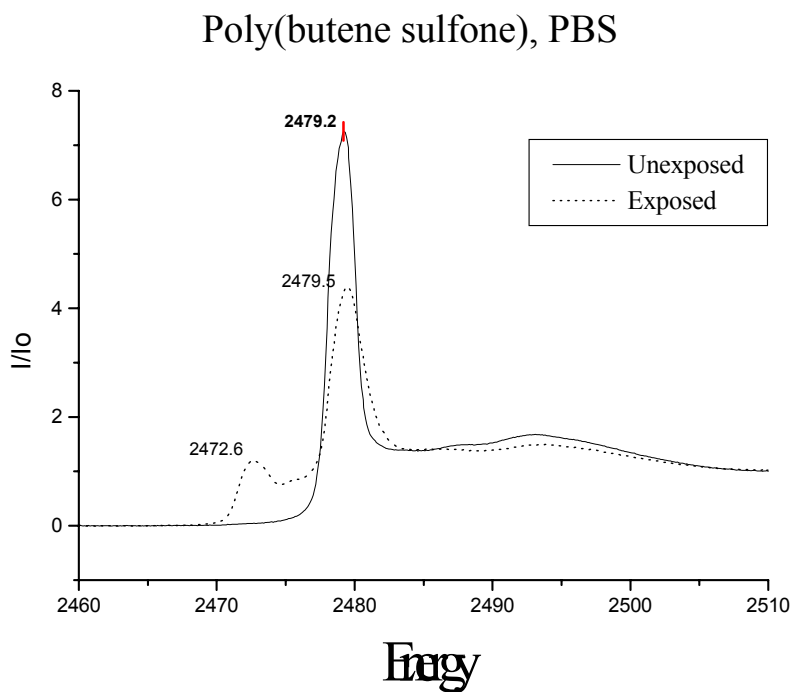


Figure 2.1 An x-ray absorption spectrum showing the sulfur K-edge XANES of PBS

The photon energy at which the maximum of the absorption spectrum occurs gives electronic information of the absorbing atom. For example, a shift of the peak to a lower energy indicates a change in the atom to a more reduced state. Alternately, a shift to a higher energy represents a change to a more oxidized state. Figure 2.1 shows the

XANES spectrum for the sulfur K-edge of PBS before and after irradiation with x-rays. Before irradiation, a peak is seen at 2479.8 eV, representing the state of the sulfur atom as a sulfone (SO₂), derived by comparison to several reference compounds.^{8,11} The XANES spectrum of irradiated PBS gives two peaks: one at 2479 eV indicating the presence of sulfone, and a peak at 2472.6 eV indicating the presence of a reduced sulfur species corresponding to a sulfide (S)¹¹. In the region of the spectrum past these peaks, around 2490-2510 eV, certain “shape resonances” can be observed. These shape resonances give valuable information on the environment surrounding the sulfur atom. In this study, however, we focus on the region around 2470-2485 eV.¹¹

Information on the changes occurring in the sulfur atom as a result of irradiation can be a useful tool in understanding chain scission pathways. The information gathered from the XANES spectra of various polysulfones can be used to hypothesize possible mechanisms involved in their degradation.

2.1.2 Measurement of x-ray absorption

X-ray absorption spectra can be obtained from several different types of measurements. Transmission measurements are made by determining the fraction of the incident x-ray beam transmitted through a sample. The reciprocal of this transmitted fraction is proportional to the logarithm of the absorption coefficient (Beer’s law). Alternatively, one can use fluorescence measurements, in which one measures the intensity of radiation emitted from a sample when electrons from outer shells of an atom drop down to occupy vacancies in inner shells caused by the x-ray absorption process. In this case, the intensity of the fluorescence is proportional to the extent of absorption of the incident radiation. Another type of measurement is the detection of the total emission

of electrons from the element of interest in the sample resulting from the x-ray absorption process. The measured “total electron yield” is then proportional to the extent of x-ray absorption. This method of measurement is convenient to use to eliminate sample “thickness effects” which are important considerations in both transmission and fluorescence techniques.⁶

2.1.3 Experimental

2.1.3.1 Sample preparation and exposure.

Thin films (~3 μm) of each of the polymers were spin-coated onto 4” silicon wafers. The samples were then exposed to soft x-rays ($\lambda = 8\text{-}10$ Angstroms) generated from the synchrotron facility, CAMD (Center for Advanced Microstructures & Devices) at LSU. Exposures were performed under a vacuum pressure of 10^{-4} to 10^{-5} Torr at the XRLC1 beamline. The XRLC1 beamline is comprised of a series of mirrors and filters to select the desired band of energy from the synchrotron. A beryllium window excludes all UV and visible radiation, allowing only x-rays to pass. Past that, two mirrors act to cut off the higher energy x-rays, resulting in a beam of approximately 8-10 Angstroms wavelength of light. The exposure dose for all the samples was 50 mJ/cm^2 . XANES data was obtained both before and after exposure to x-rays.

2.1.3.2 XANES

XANES spectra were collected at the DCM1 beamline at CAMD. The DCM1 beamline uses a double crystal monochromator to collimate the x-ray beam to a narrower bandwidth. The photon energy range used to obtain the XANES spectrum for the sulfur K-edge was around 2450-2510 eV. A Total Electron Yield (TEY) detector was used to measure the signal, and an ionization chamber was used to monitor I_0 . Both were

operating at 100 mbar He. The maximum of the spectral line of ZnSO_4 at 2481.44 eV was used for energy calibration. A zero point (E_0) on the energy scale was chosen, which corresponded to the inflection point in the edge of the sulfone spectral white line.

XANES data were obtained and reduced by doing a background removal, which was based on the difference of absorption values obtained by extrapolation of the data from the pre-edge and post-edge regions of the TEY/I_0 spectrum.

2.1.3.3 Results

The sulfur K-edge XANES of several reference compounds are shown in Figure 2.2.⁸ The XANES results for the polymers are given in Figures 2.3 and 2.4. In the spectra of the unexposed samples, the presence of the sulfone group (SO_2) is indicated by the large peak, located around 2479 eV. It is interesting to note that the sulfone peak for polysulfone resin (PSR) is slightly shifted to higher photon energy around 2480 eV. This can be attributed to the presence of the aromatic groups on either side of the SO_2 group, which offer a delocalized pi electron system.

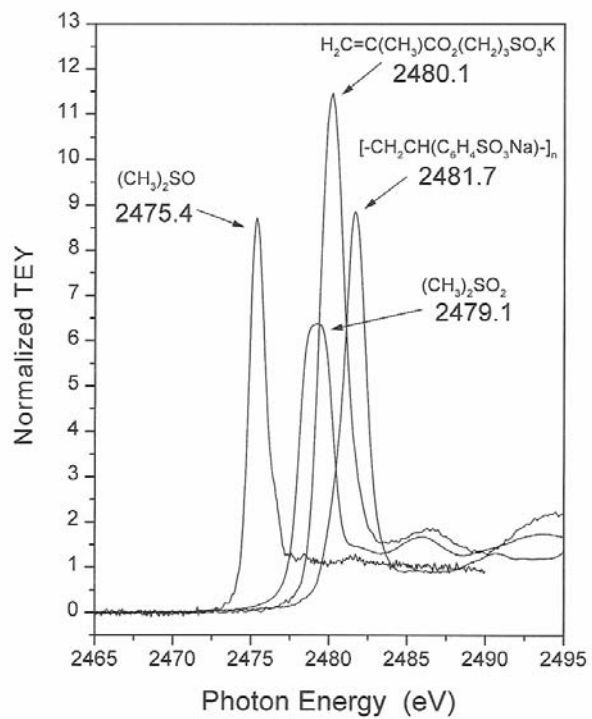
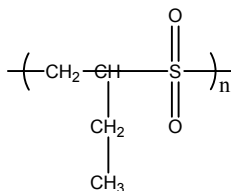
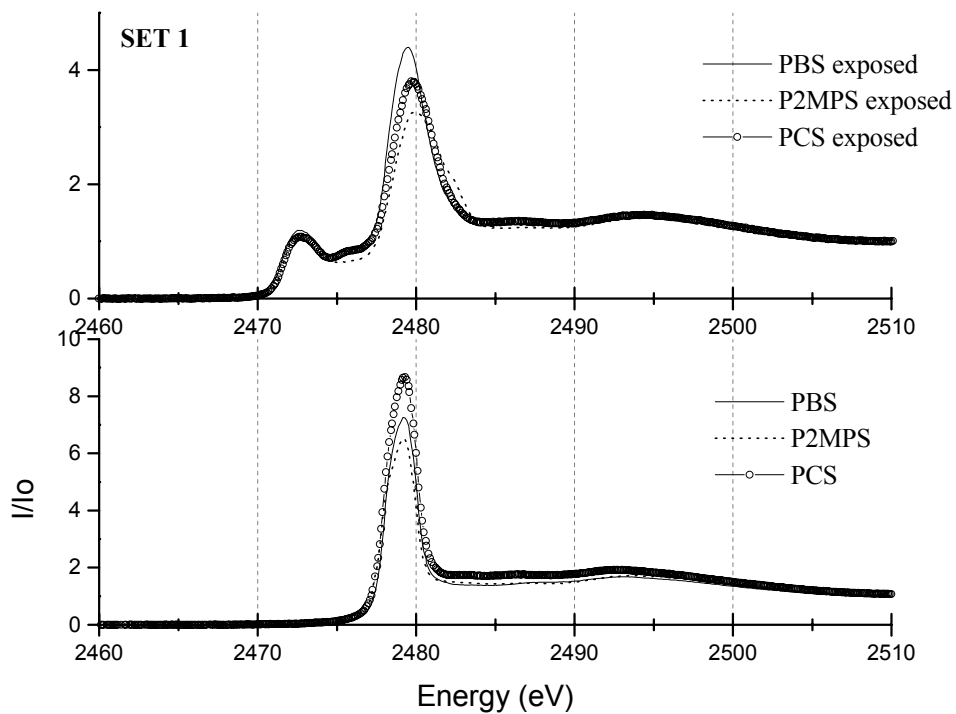
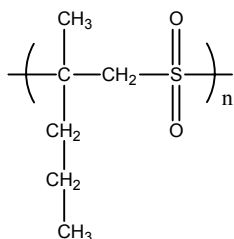


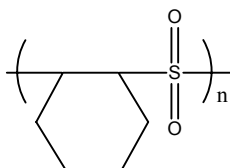
Figure 2.2 Sulfur K-edge XANES of reference compounds.



Poly(butene sulfone)
PBS



Poly(2-methyl pentene sulfone)
P2MPS



Poly(cyclohexene sulfone)
PCS

Figure 2.3 XANES results of poly(olefin sulfones)

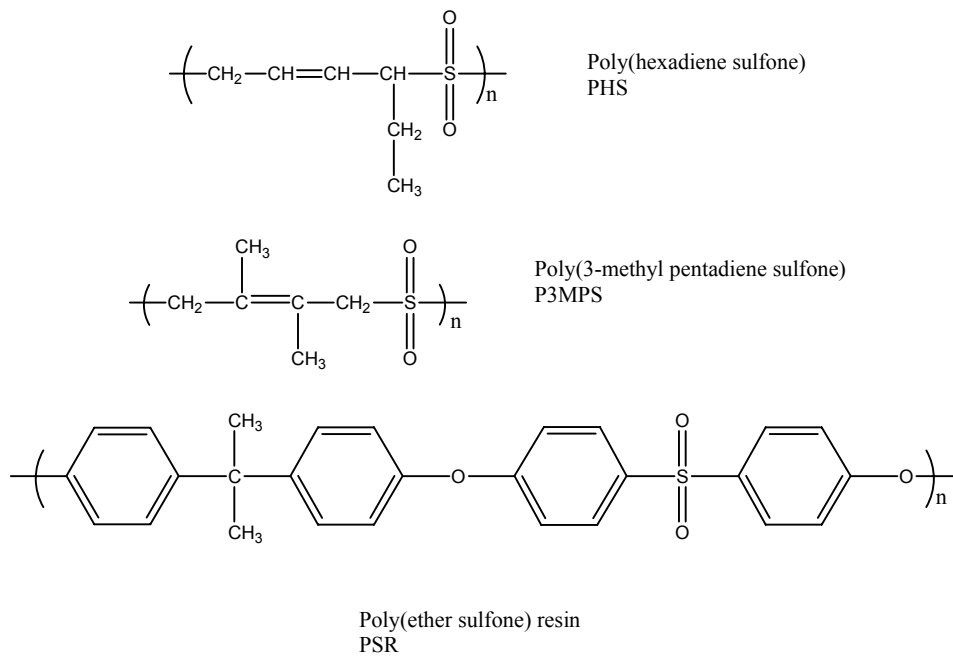
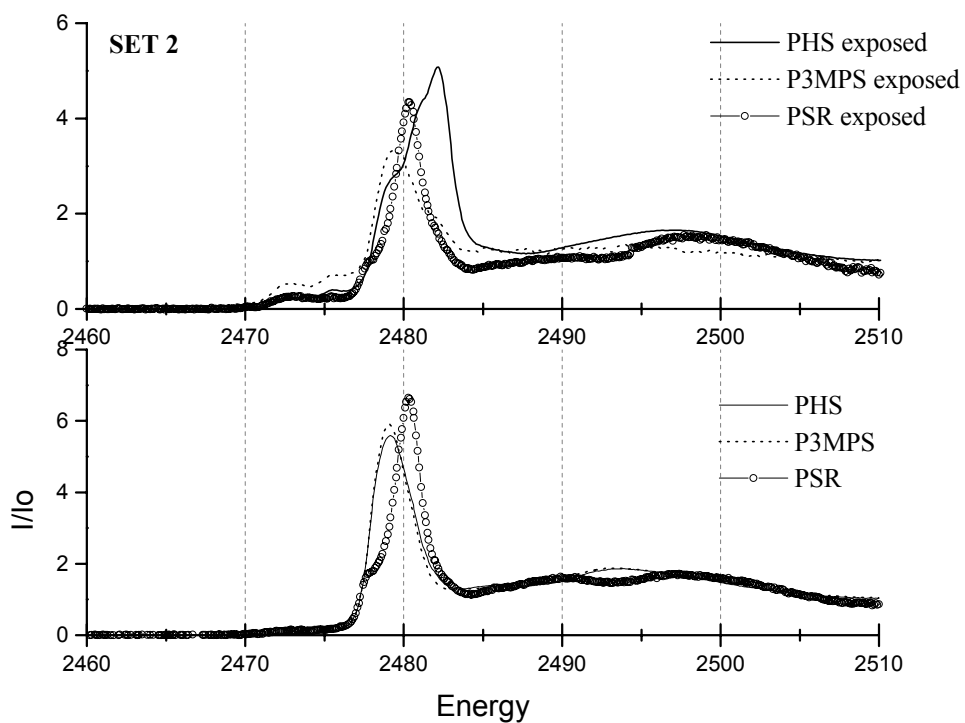


Figure 2.4 XANES results of poly(unsaturated olefin sulfones)

In the spectra of the exposed samples, it can be seen that the intensity of the sulfone group has decreased and new peaks have developed. This indicates a decrease in the amount of SO₂ groups and the formation of new sulfur states within the polymer, resulting from irradiation. With the exception of polysulfone resin (PSR), all of the polysulfones show a slight shift of the sulfone peak towards higher photon energy by about 0.3 to 0.5 eV, indicating movement towards a more oxidized state. The spectrum of irradiated PSR shows no shift of the sulfone peak and no formation of new sulfur states, although the sulfone peak does appear to have decreased in intensity. Aromatic groups are known to exhibit resistance to radiation; this is confirmed by the failure to observe any changes in the spectrum of irradiated PSR.

It is interesting to note the similarities in the spectra of polymers with similar chemical structures, particularly the presence or absence of a C=C in the backbone. It appears as though the polysulfones lacking a C=C in the backbone exhibit a pronounced peak around 2473 eV after irradiation (Figure 2.3). This peak can be attributed to a sulfide group (S), based upon the reference peak of dimethyl sulfide at 2472.5 eV. PBS and P2MPS have very similar structures. The SO₂ group in PBS is bound to a primary CH₂ group and a secondary CH group. P2MPS has an SO₂ group bound to a primary CH₂ and a tertiary C with a slightly longer chain. PCS has an SO₂ group bound to a cyclohexane secondary CH on either side, and exhibits the same sulfide peak after irradiation.

On the other hand, the polysulfones PHS and P3MPS which have a C=C in their backbone, have spectra that are more difficult to assess (Figure 2.4). The spectrum of irradiated P3MPS shows a decreased intensity in the SO₂ peak and possibly two very

small peaks around 2473 and 2475 eV which represent more reduced sulfur species. The peak at 2473 eV can be assigned as the sulfide (S) peak, and the peak at 2475 eV as a sulfoxide (SO) in conjunction with the reference dimethyl sulfoxide. In addition, there appears to be a developing peak around 2482 eV, representing a more oxidized state. This state has been speculated to be either a sulfonate (SO₃) or sulfate (SO₄). The spectrum of irradiated PHS also appears to have two small peaks developing around 2473 and 2475 eV, as well as a pronounced peak around 2482 eV.

In a 1998 publication⁹, we reported a XANES study performed on PBS and PHS, exposed with a range of dosages. These results correlate with the data in Figures 2.3 and 2.4. It was found for PHS that as the dosage increased, the peak at 2482 eV increased in intensity, indicating the breaking of a S-C bond to generate either the SO₃ or SO₄ state of sulfur. In contrast, the peak at 2482 eV is absent in the spectrum of PBS, even at high dosages. It was proposed that the presence of the C=C in PHS is responsible for the generation of the more oxidized state of sulfur.⁹ The presence of a developing peak at 2482 eV in the spectrum of irradiated P3MPS, which also contains a C=C, supports this postulate.

2.2 In Situ Mass Spectrometry of Irradiated Poly(olefin sulfones)

2.2.1 Introduction

The detection of vaporized species produced during irradiation of a polymer can give insight to its photochemical behavior. The high sensitivity of polysulfones to radiation can be attributed to their mechanism of chain scission. Irradiation causes main chain scission, which initially occurs at the relatively weak sulfur-carbon bond, generating SO₂. Another aspect which contributes to their high sensitivity is their very

low ceiling temperature (T_c), the temperature for which the rate of monomer addition is equal to the rate of depolymerization. The low T_c of polysulfones makes them unstable at room temperature, so one chain scission initiated at room temperature causes rapid depolymerization, or unzipping, of the chain. In the case of positive photoresists, main chain scission results in a decrease in the molecular weight of the polymer and a subsequent increase in its solubility in appropriate solvents. In some cases, irradiation results in the complete transformation of the polymer to volatile products, leading to a form of self-development exhibited by polysulfones.^{3,5} In situ mass spectrometry is a valuable tool in the detection of such volatile species.^{8,10}

An example of a well-known mechanism elucidated by in situ mass spectrometry is that of PMMA degradation resulting from UV irradiation. The mass spectra of the vaporized products were interpreted to give possible degradation reactions of PMMA as a result of UV irradiation (Figure 2.5). It was concluded that UV absorption at the C=O unit results in side chain scission to generate the products shown by the peaks at 59 and 31 amu. The peaks at 41 and 69 amu are due to main chain scission initiated by side chain scission.⁶

In situ mass spectrometry was also used to analyze the radiation chemistry of a novel resist comparable to PMMA for LIGA applications at the University of Bonn in Germany. Results of their experiments showed similar main chain scissions at the CO₂ group. The typical mass spectrum of the poly(L-lactide) under irradiation gave major peaks at 28 and 44 atomic mass units. The peak at 28 amu was assigned to include about 90% CO and 10% C₂H₄, while the peak at 44 amu was assigned to include about 80% CO₂ and 20% HCOCH₃. With the aid of the mass spectrum in combination with IR

spectra, they were able to arrive at a radiation degradation mechanism given in Figure 2.6.¹⁰

Our goal is to use the results of mass spectrometry in combination with XANES to determine a possible mechanism for the radiation-induced degradation of the poly(diene sulfones) mentioned in Chapter 1.

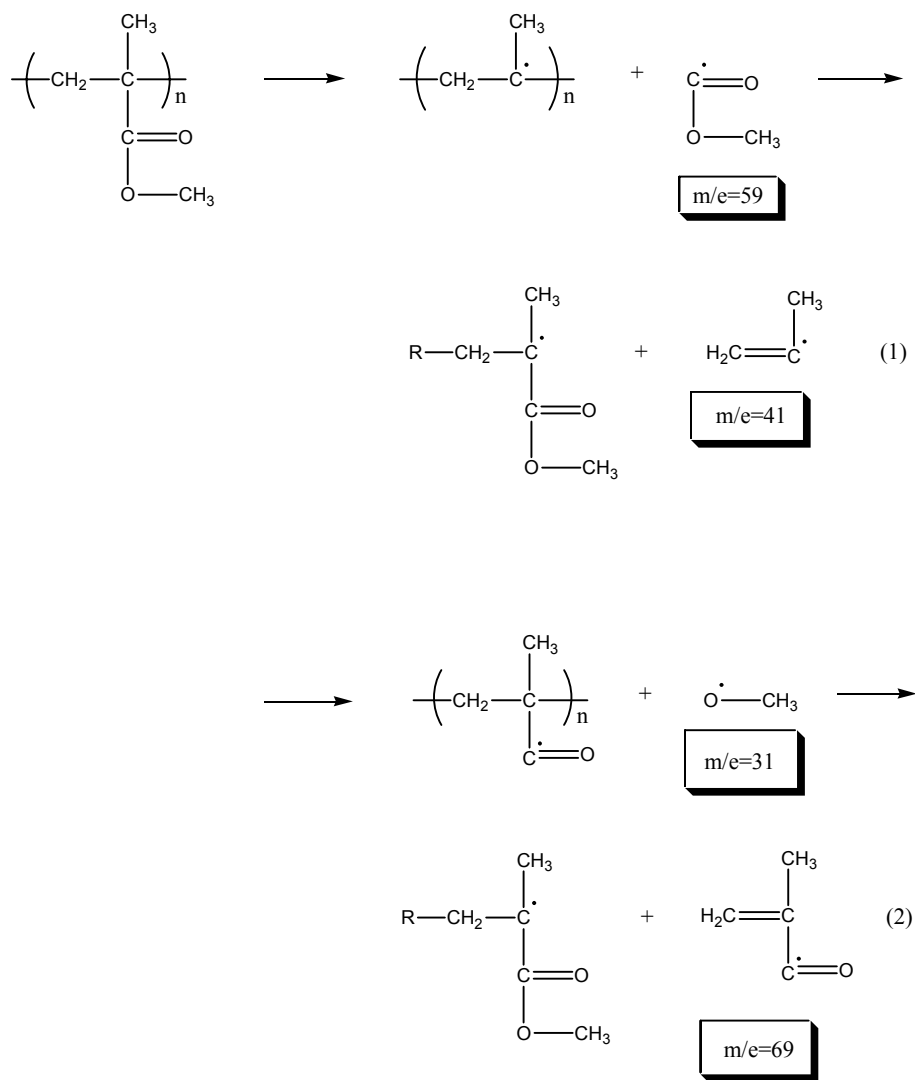


Figure 2.5 UV degradation products of PMMA detected with in situ mass spectrometry.

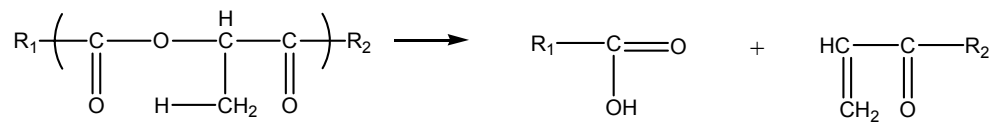


Figure 2.6 Radiation degradation mechanism of poly(lactide)

2.2.2 Experimental

2.2.2.1 Set-up and procedure

A diagram of the experimental set-up is given in Figure 2.7. The mass spectrometer used for this experiment was a Stanford Research Systems Residual Gas Analyzer, RGA Model#100. It was mounted onto the sample exposure chamber at the end of the XRLC1 beamline. Another chamber housing a filter that blocked the x-rays was placed between the beamline and the sample chamber. A gate valve separated the filter chamber from the sample chamber, and both chambers were pumped down to a vacuum pressure of approximately 10^{-4} Torr before the gate valve was opened between them. Gate valves also separated the filter chamber from the end of the beamline, and the front end of the beamline from the synchrotron. Before the gate valve was opened between the two chambers, the filter was lowered to completely block all x-rays. A background spectrum was obtained in the sample chamber. Then the filter was manually raised until a spot of x-rays hit the sample. A spectrum was taken immediately at the point of exposure.

The Residual Gas Analyzer (RGA) analyzes residual gases by ionizing some of the gas molecules into positive ions by bombarding them with electrons derived from a heated filament. The ions are then transferred from the ionizer into the quadrupole where they are filtered according to their mass-to-charge ratio. The ions that pass through the filter are then focused towards the detector, which measures the ion currents directly.

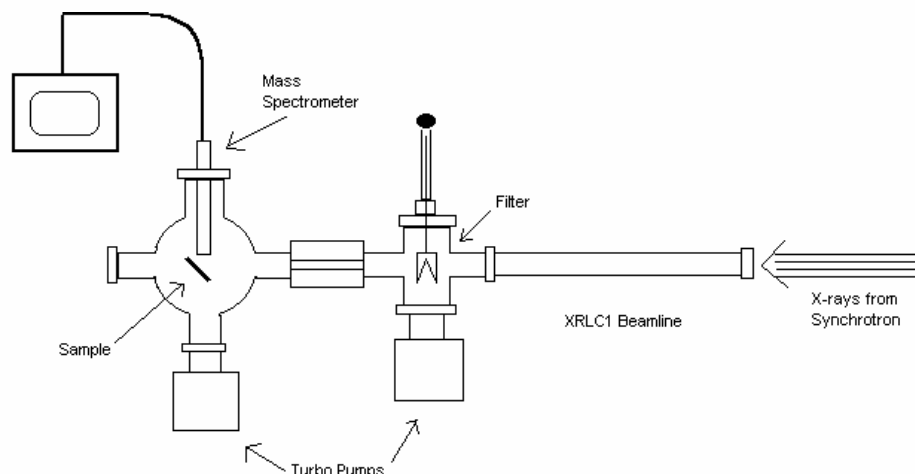


Figure 2.7 Experimental set-up of the mass spectrometer.

2.2.2.2 Results

The results are given in Figures 2.8, 2.9 and 2.10. The data were corrected by subtracting the background residual gas spectrum obtained before irradiation of the sample. A set of molecular fragments can be considered for each of the peaks. The peaks at 65 and 49 amu can be assigned to SO_2 and SO respectively. Several of the other main peaks are assigned possible molecular ion fragments, which are shown with the data. Other possible fragments are given in Table 2.4.

As with the XANES spectra, there appear to be similar trends in the mass spectra of polysulfones with similar chemical structures. During the irradiation of both PBS and P2MPS, an abundance of different gaseous species were detected (Figure 2.8). Similarly, the spectrum for PCS shows the generation of many of the same gaseous species occurring at 65, 49, 42, 40 and 28 atomic mass units (amu) (Figure 2.10). P3MPS and PHS have strikingly similar mass spectra, indicating the presence of two major species at 65 and 49 amu, and a minor one at 33 amu (Figure 2.9). Even more interesting is the lack

of any other ion fragments in the spectra of these two polymers. The spectrum of PSR shows no additional peaks during irradiation, in agreement with its resistance to radiation.

2.3 Discussion of Spectroscopic Results

The XANES spectra were obtained on the samples before exposure to radiation and again after they were exposed to a dose of 50 mJ/cm². The mass spectra were obtained during exposure with no filters to modify the incident radiation. Therefore, an actual dose cannot be assigned to the radiation. Furthermore, the XANES data and the mass spectral data cannot be compared on the basis of irradiation dose.

The main volatile products detected during the irradiation of PBS and P2MPS were very similar. PBS and P2MPS both have polymer backbones that lack a C=C. Both polymers generate several ion fragments of 65, 57, 49, 42, 40 and 28 atomic mass units. Table 2.3 lists some masses and their corresponding molecular ion fragments. The peaks at 65 and 49 amu can be assumed to be HSO₂ and HSO. The peak at 57 amu typifies a C₄ fragment, and the peaks at 42 and 40 amu could indicate C₃ fragments. The peak at 28 amu could either be a C₂ fragment or CO.

PBS, a commercial e-beam resist, has been studied and a pathway for its radiation degradation has been suggested. Irradiation activates the labile S-C bond resulting in the liberation of SO₂ and the generation of 1-butene monomer (C₄). The mechanism is given in Figure 2.11. One of the major peaks in the mass spectrum of PBS (65 amu) indicates the liberation of SO₂. The other major peak (42 amu) indicates a larger presence of C₃ fragments. In addition, the abundance of C₄ fragments (57 amu), though present, is comparably small. These results can be interpreted based on the known mechanism of the degradation of PBS. They show that after the polymer chain has been essentially

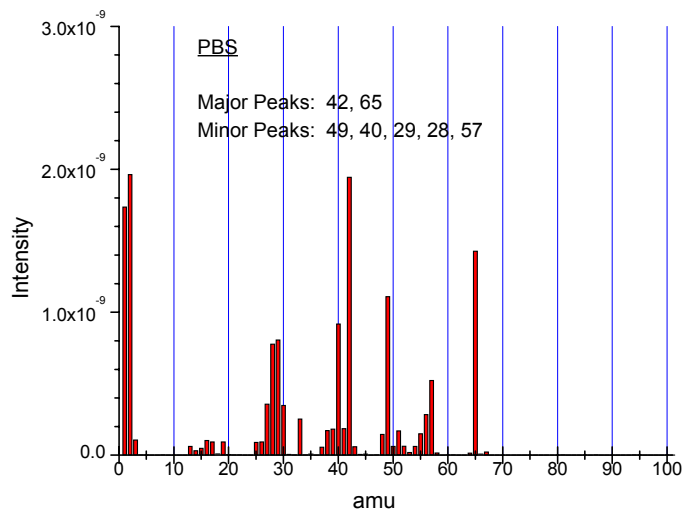
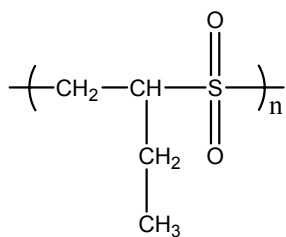
depolymerized into the butene monomer and SO₂, the subsequent reactions involve mainly the fragmentation of the monomer into smaller moieties, specifically into C₃ fragments.

2.3.1 Poly(butene sulfone) and Poly(2-methyl pentene sulfone)

The mass spectrum of P2MPS can be explained similarly. It too indicates a large abundance of HSO₂ (65 amu). Other major peaks include C₄ and C₃ fragments (57, 42 and 40 amu), as well as amounts of C₂ or CO fragments (28 and 30 amu). P2MPS has a longer alkyl side chain and a 3° carbon, which may generate a larger possibility of alkane fragments. In addition to these lower molecular weight ions, there exist some heavier C₅ and C₆ fragments, indicated by the peaks at 70 and 85 amu. The detection of an abundance of HSO (49 amu) in the mass spectrum of both polymers is difficult to assess. Its abundance is slightly less than that of HSO₂, but large enough to be considered a major product. Perhaps it is due to the reduction of gaseous SO₂.

The XANES spectra of PBS and P2MPS are also very similar. After irradiation with a dose of 50mJ/cm², there is a smaller amount of SO₂ and the presence of sulfide (S) in the polymer. This indicates that at the given dose, the sulfur atom becomes reduced. However it is not known whether actual chain scission has occurred. It can be speculated that the reduction of sulfur initiates the process leading towards chain scission and liberation of SO₂.

PBS



P2MPS

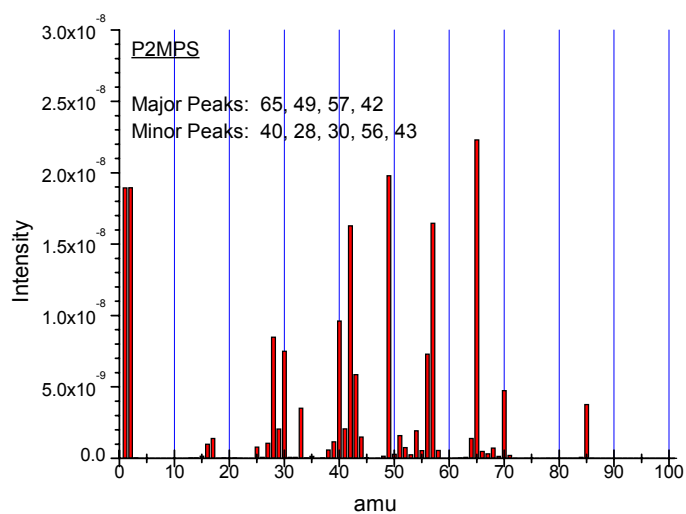
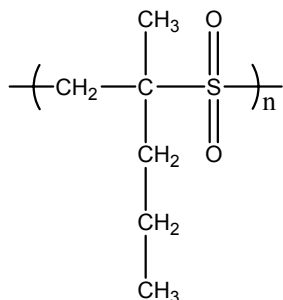


Figure 2.8 Mass spectrometry results of poly(olefin sulfones)

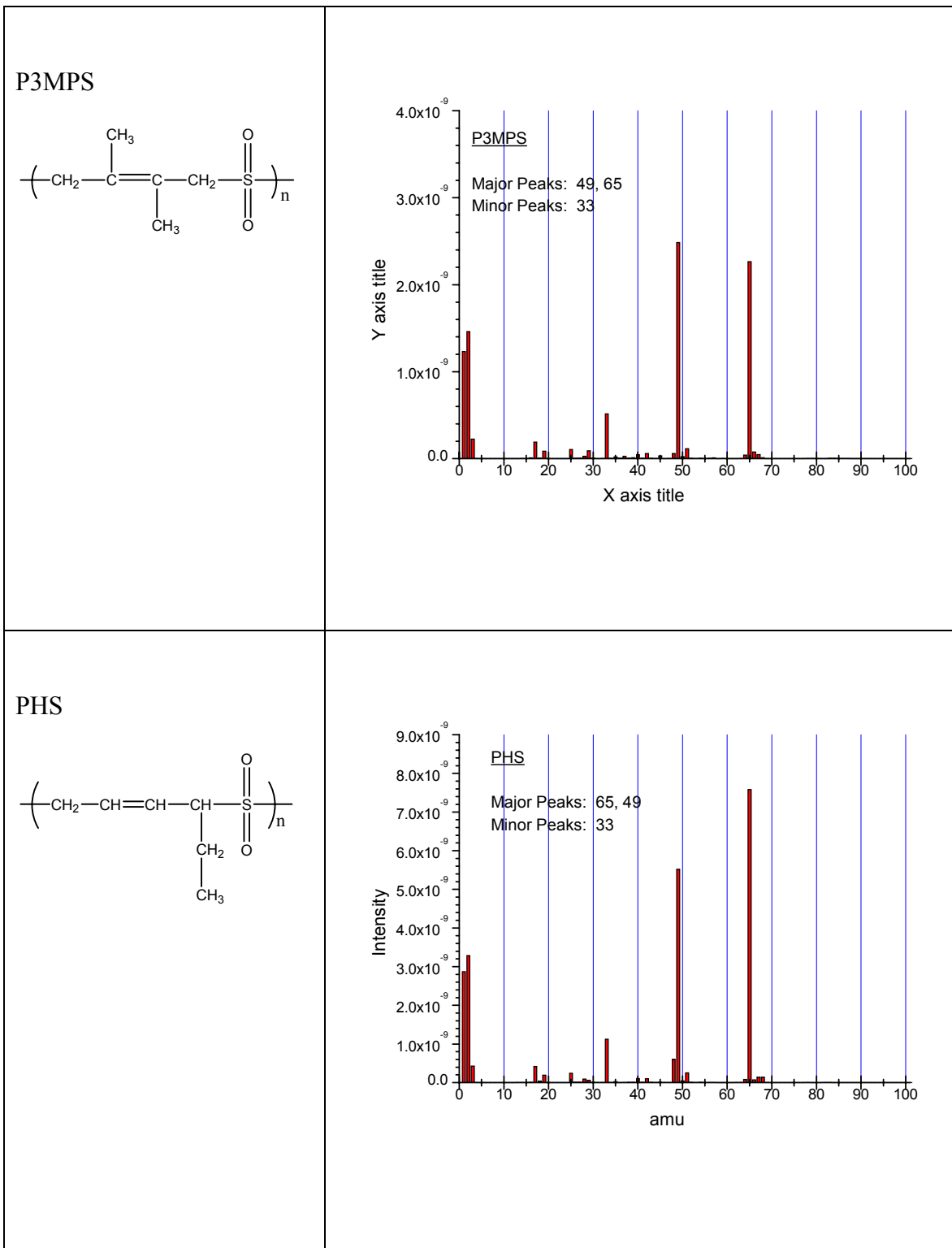


Figure 2.9 Mass spectrometry results of poly(unsaturated olefin sulfones)

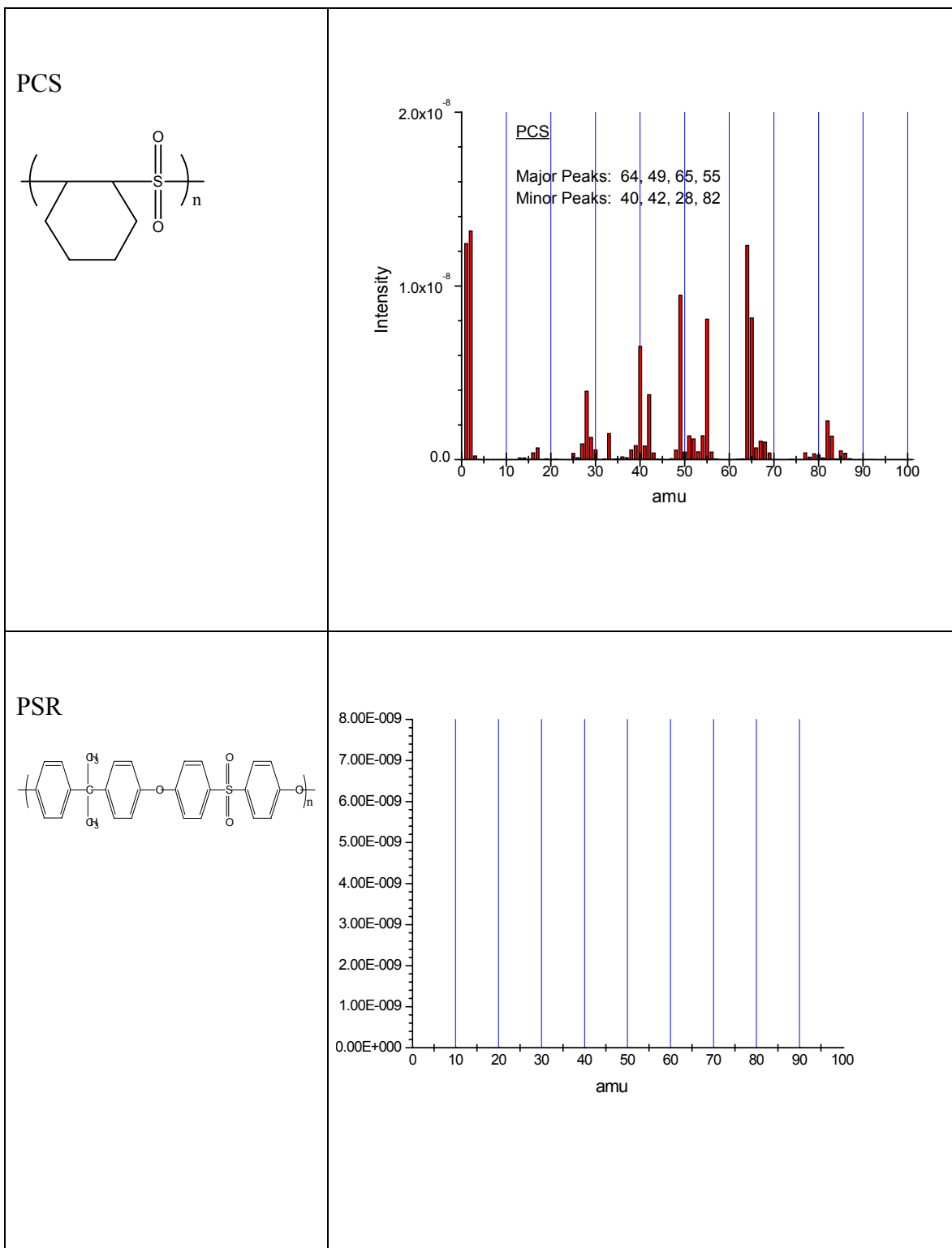


Figure 2.10 Mass spectrometry results for poly(cyclic aliphatic or aromatic sulfones)

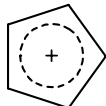
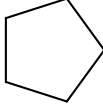
Mass	Fragments		
m/z = 28	$\text{H}_2\text{C}=\text{CH}_2$	$\text{C}\equiv\text{O}^+$	
m/z = 29	$\text{H}_3\text{C}-\text{CH}_2^+$	$\text{HC}\equiv\text{O}^+$	
m/z = 30	$\text{H}_3\text{C}-\text{CH}_3$	$\text{H}_2\text{C}=\text{O}^+$	
m/z = 33	S^+-H	$\text{H}_3\text{C}-\text{OH}_2^+$	
m/z = 40	$\text{H}_2\text{C}=\text{C}=\text{CH}_2$		
m/z = 41	$\text{H}_2\text{C}=\underset{\text{H}}{\text{C}}-\text{CH}_2^+$		
m/z = 42	$\text{H}_2\text{C}=\underset{\text{H}}{\text{C}}-\text{CH}_3$	$\text{H}_3\text{C}-\text{C}^+-\text{CH}_3$	$\text{H}_2\text{C}=\text{C}=\text{O}^+$
m/z = 43	$\text{H}_3\text{C}-\underset{\text{H}}{\text{C}}^+-\text{CH}_3$	$\text{H}_3\text{C}-\text{C}\equiv\text{O}^+$	
m/z = 49	$\text{HS}^+=\text{O}$		
m/z = 55	$\text{H}_2\text{C}=\underset{\text{H}}{\text{C}}-\underset{\text{H}}{\text{C}}^+-\text{CH}_3$	$\text{H}_2\text{C}=\underset{\text{H}}{\text{C}}-\text{C}\equiv\text{O}$	
	$\text{H}_2\text{C}=\text{C}^+-\underset{\text{H}_2}{\text{C}}-\text{CH}_3$		
m/z = 56	$\text{H}_3\text{C}-\underset{\text{H}}{\text{C}}=\underset{\text{H}}{\text{C}}-\text{CH}_3$	$\text{H}_2\text{C}=\underset{\text{H}}{\text{C}}-\underset{\text{H}}{\text{C}}=\text{O}^+$	
m/z = 57	$\text{H}_3\text{C}-\underset{\text{H}}{\text{C}}^+-\underset{\text{H}_2}{\text{C}}-\text{CH}_3$	$\text{H}_2\text{C}=\underset{\text{H}}{\text{C}}-\underset{\text{H}}{\text{C}}=\text{OH}^+$	$\text{H}_3\text{C}-\overset{\text{CH}_3}{\underset{\text{H}_2}{\text{C}}^+-\text{CH}_3$
m/z = 64	$\text{O}=\text{S}^+=\text{O}$	$\text{H}_3\text{C}-\text{S}^+=\text{OH}^+$	
m/z = 65	$\text{O}=\text{S}^+=\text{OH}^+$		

Table 2.1 List of mass peaks and their corresponding molecular ions. (Table continued)

m/z = 70	$\begin{array}{ccccccc} \text{H}_2\text{C} & = & \text{C} & - & \text{C} & - & \text{C} & - & \text{CH}_3 \\ & & \text{H} & & \text{H}_2 & & \text{H}_2 & & \end{array}$ $\begin{array}{ccccccc} \text{H}_3\text{C} & - & \text{C} & = & \text{C} & - & \text{C} & - & \text{CH}_3 \\ & & \text{H} & & \text{H} & & \text{H}_2 & & \end{array}$ 
m/z = 85	$\begin{array}{ccccccc} & & & & \text{CH}_3 & & & & \\ & & & & & & & & \\ \text{H}_3\text{C} & - & \text{C} & - & \text{C} & - & \text{C} & - & \text{CH}_3 \\ & & \text{H}_2 & & \text{H}_2 & & \text{C}^+ & & \end{array}$ $\text{H}_3\text{C} - \text{C}^+ - \text{C} - \text{C} - \text{C} - \text{CH}_3$ $\begin{array}{ccccccc} & & & & & & & & \\ & & & & \text{H} & & \text{H}_2 & & \text{H}_2 & & \text{H}_2 & & \\ & & & & & & & & & & & & \end{array}$

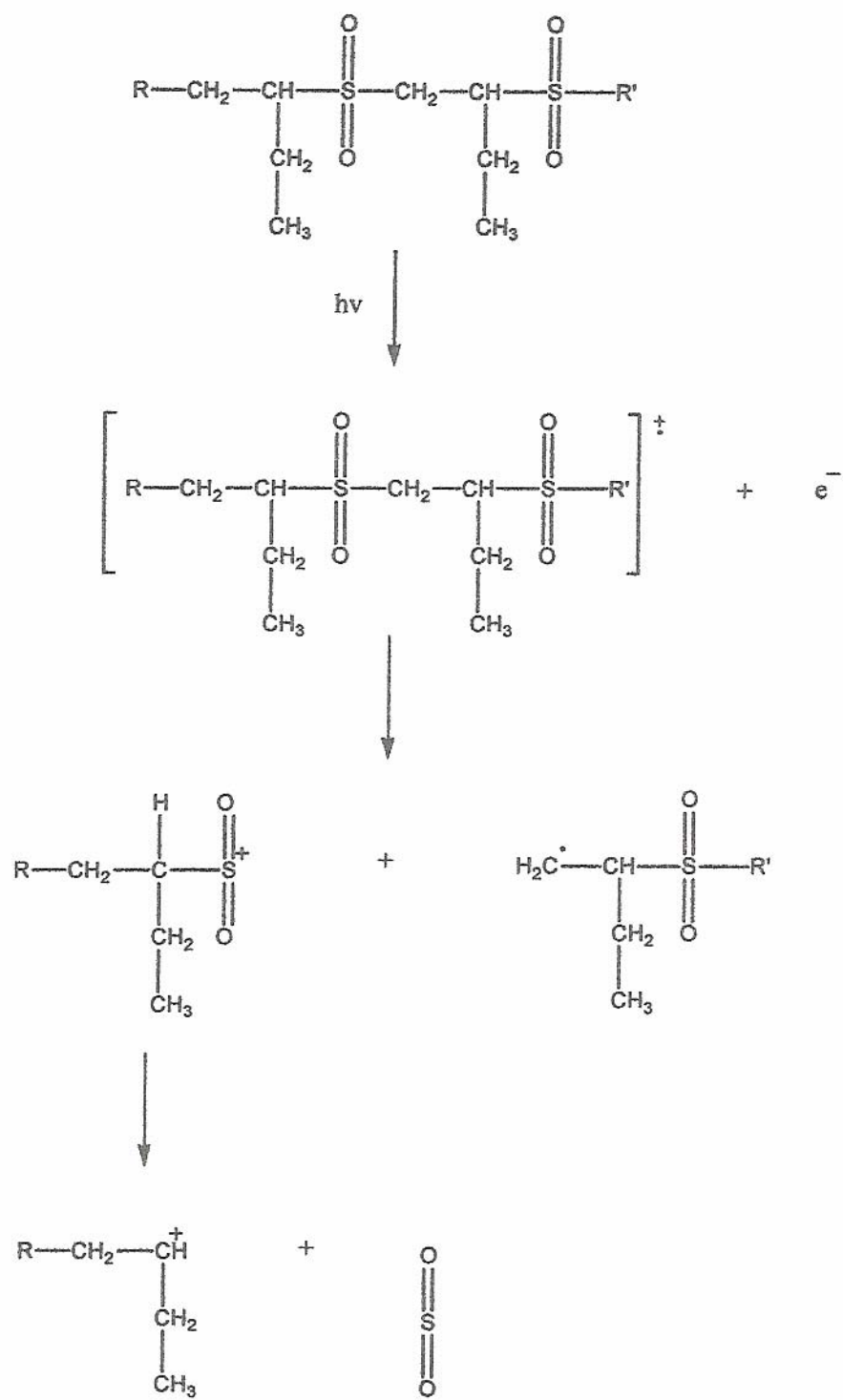


Figure 2.11 Decomposition pathway of PBS

2.3.2 Poly(3-methyl pentadiene sulfone) and Poly(hexadiene sulfone)

P3MPS and PHS both have a polymer backbone that contains a C=C bond. The mass spectra show only two main gaseous species evolving from the polymer during irradiation, HSO₂ and HSO (65 and 49 amu). This suggests that irradiation by high-energy x-rays causes chain scission at the S-C bond with the liberation of SO₂ and SO as the major volatile products. A species, which could be HS (33 amu), is produced in small amounts. It appears that chain cleavage results in the generation of a stable species, which does not further unzip. Since there are no molecular ion fragments detected above 65 amu, it can be assumed that the resulting lower molecular weight oligomer is a non-volatile species. The presence of a conjugated pi electron system in the diene appears to offer a stabilizing effect on the oligomer. It is not clear what the role of HSO is in the degradation process, or whether it is a result of the reduction of SO₂ and further reduced to S, or some other pathway.

The XANES spectra of P3MPS and PHS are also similar. After irradiation, two very tiny peaks in the spectra indicate the presence of reduced sulfur groups, sulfide (S) and sulfoxide (SO). In addition, there appears to be another peak indicating a more oxidized sulfur group, SO₃ or SO₄. It is interesting to note that the peak for the more oxidized sulfur species (indicating SO₃ or SO₄) is more significant in exposed PHS than P3MPS, whereas the peaks for the more reduced species (indicating S and SO) are more prominent in exposed P3MPS than PHS.

In an earlier study done on PHS and PBS, XANES spectra showed that PHS, exposed with a dose of 50 mJ/cm², exhibited a peak at 2482 eV indicating a more oxidized sulfur species (SO₃ or SO₄). Figure 2.12 shows the results. As the exposure dose

was increased on PHS, the peak increased in intensity. PBS did not exhibit this peak, even after exposure to high dosages. It was suggested that the presence of the C=C bond in the PHS has a significant effect on its reactivity to x-rays, i.e. the oxidation of SO₂ to SO₃ or SO₄.⁸ In this study P3MPS, exposed at a dose of 50 mJ/cm², begins to show the same SO₃ or SO₄ peak, supporting this claim.

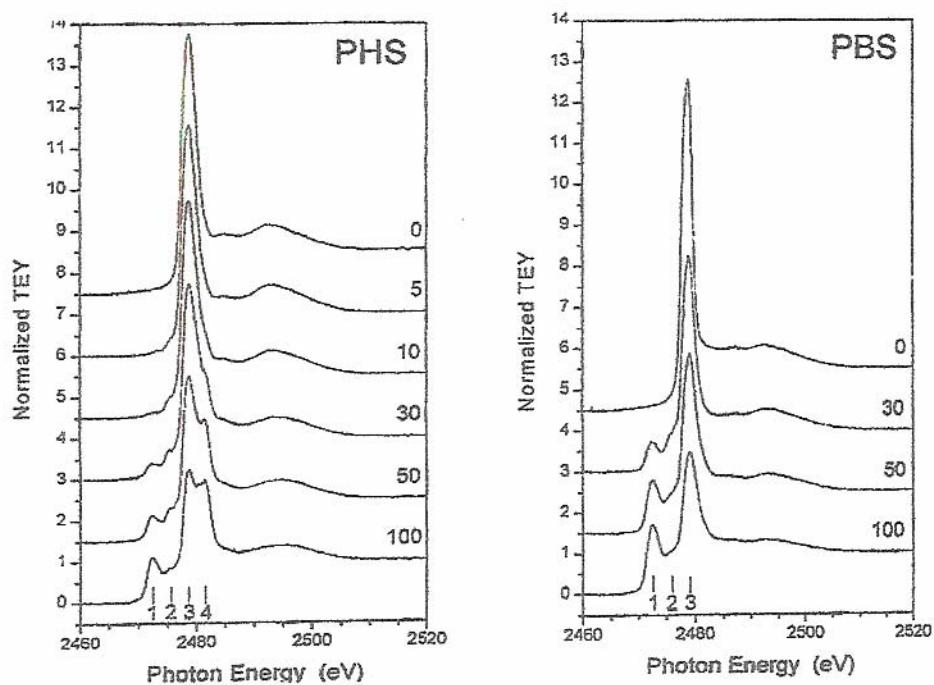


Figure 2.12 Sulfur K edge XANES of PHS and PBS at increasing doses.

CHAPTER 3

SYNTHESIS OF POLY(PENTADIENE SULFONE) AND POLY(HEPTADIENE SULFONE)

3.1 Introduction

The synthesis of poly(pentadiene sulfone) and poly(heptadiene sulfone) will be attempted through a radical co-polymerization. This method includes the processes of initiation, propagation and termination. Initiation involves the introduction of a radical species, which attacks a monomer molecule, transforming it into another radical. A common source for initiation in radical polymerization is peroxide decomposition. Initiation is followed by propagation, where the radical monomer adds to other monomers, forming a growing polymer chain. Termination occurs when a radical is removed from the system by reacting with another radical. The interplay of initiation, propagation and termination determines the outcome of the polymerization reaction and the properties of the resulting polymers.¹³

In the polymerization of olefins, addition usually occurs in a head-to-tail fashion, where the radical attacks from the CH₂ end of the double bond leading to a radical moiety on the adjacent substituted carbon atom. Figure 3.1 illustrates the 1,2 addition of a radical with an olefin. The copolymerization of SO₂ with 1,3 dienes occurs via the 1,4 addition mechanism shown in Figure 3.2.³

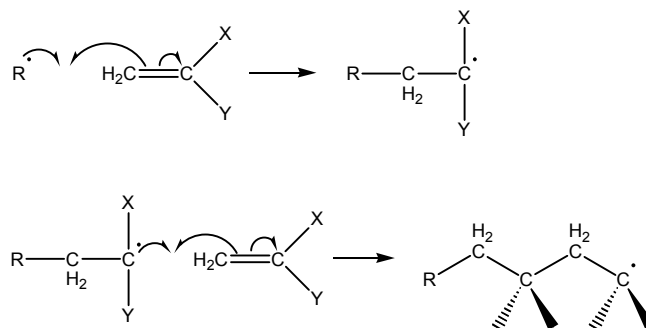


Figure 3.1 1,2 addition polymerization

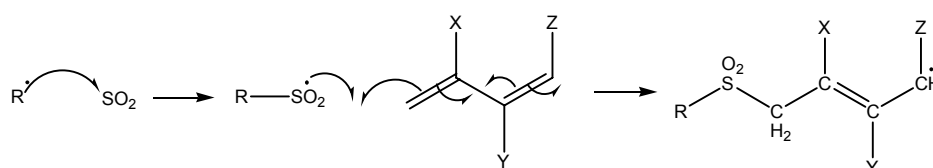


Figure 3.2 Copolymerization of 1,3 dienes with SO₂

3.2 Synthesis of Poly(pentadiene sulfone), PPS

3.2.1 Procedure

The monomer, 1,3-pentadiene, was purchased from Aldrich Chemical Company and used as received. The sulfur dioxide was contained in a gas cylinder, also purchased from Aldrich. The initiator for the polymerization was t-butyl hydroperoxide. The solvent for the monomer was distilled 2-nitropropane, and the solvent for the polymer was nitromethane. Methanol was used as the precipitating agent, and argon was used to purge the system.

The polymerization set-up consisted of a 3-neck 100 mL round bottom flask, with a dry ice condenser attached to the center neck. One neck opening was closed with a glass stopper. The other neck opening was covered with a rubber septum through which

a needle connected to the gas cylinder was inserted. The round bottom flask was placed in a dry ice/acetone bath to keep the temperature below -10°C .

Before setting up the system with dry ice and acetone, it was first purged with argon for approximately 30 minutes and the glassware flamed to remove air and moisture. After adding the dry ice and acetone to the condenser and bath, the system was purged an additional 15 minutes. The SO_2 gas was then condensed into the reactor and weighed. A solution of pentadiene dissolved in nitropropane was added to the condensed SO_2 in the reactor via syringe through the septum. The molar ratio of monomer to SO_2 was 1:3. The mixture was stirred until homogeneous. Approximately 1 mL of the initiator, t-butyl hydroperoxide, dissolved in about 4 mL of nitropropane, was added to the mixture via syringe through the septum. A white solid formed in the solution. The solution was allowed to warm to room temperature, then approximately 50 mL of nitromethane was added to dissolve the solid. The solid was then precipitated in approximately 500 mL of methanol, and collected. The polymer was not easily dissolved in nitromethane; it took approximately 1 week to dissolve it, with constant stirring.

The solution was expected to gel immediately after initiator was added because of the high polymerization rate. However, a white solid formed instead of gelation. Also, although approximately 0.05 mL of initiator should have been sufficient to start polymerization, as much as 1 mL was needed to begin seeing any change in the solution. This may be due to the fact that the initiator may have been old, and its potency reduced.

The results of IR analysis of the polymer are given in Figure 3.3. The peak around 1550 cm^{-1} is characteristic of the absorptions of $\text{C}=\text{C}$ stretching vibrations. The peaks at 1130 and 1300 cm^{-1} indicate the presence of a sulfone (SO_2) group.

The polymer, PPS, was fairly soluble in nitromethane; several days of stirring were required to dissolve it. The structure of the polymer consists of a double bond in the main chain and a methyl side group. The small alkyl substituent does not promote high solubility in organic solvents, in comparison to a polymer with a larger alkyl side group.

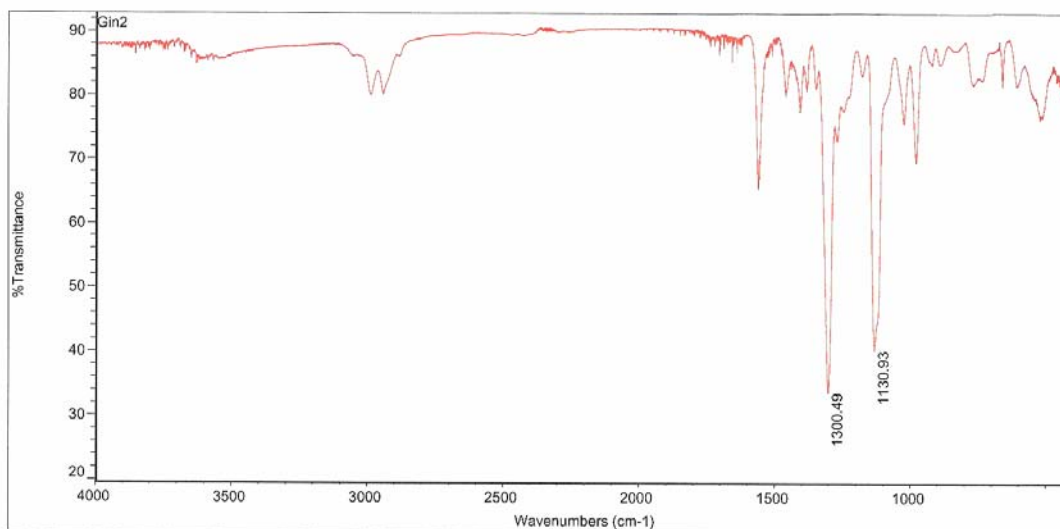


Figure 3.3 IR spectrum of PPS

3.3 Synthesis of Poly(heptadiene sulfone), PHS2

3.3.1 Monomer synthesis - The Wittig reaction

The Wittig reaction, developed in the early 1950s, has become the standard method of olefin synthesis for many reasons. The reaction is high yielding, the alkene is specifically positioned, and in many instances is stereoselective. The reaction involves the addition of a phosphonium ylide to an aldehyde to form an intermediate dipolar compound called a betaine. The betaine intermediate is unstable and decomposes at temperatures above 0°C to yield an alkene and triphenylphosphine oxide. The net result

is the replacement of carbonyl oxygen by the organic fragment originally bonded to phosphorus.¹⁴ The mechanism of the Wittig reaction is shown in Figure 3.4.

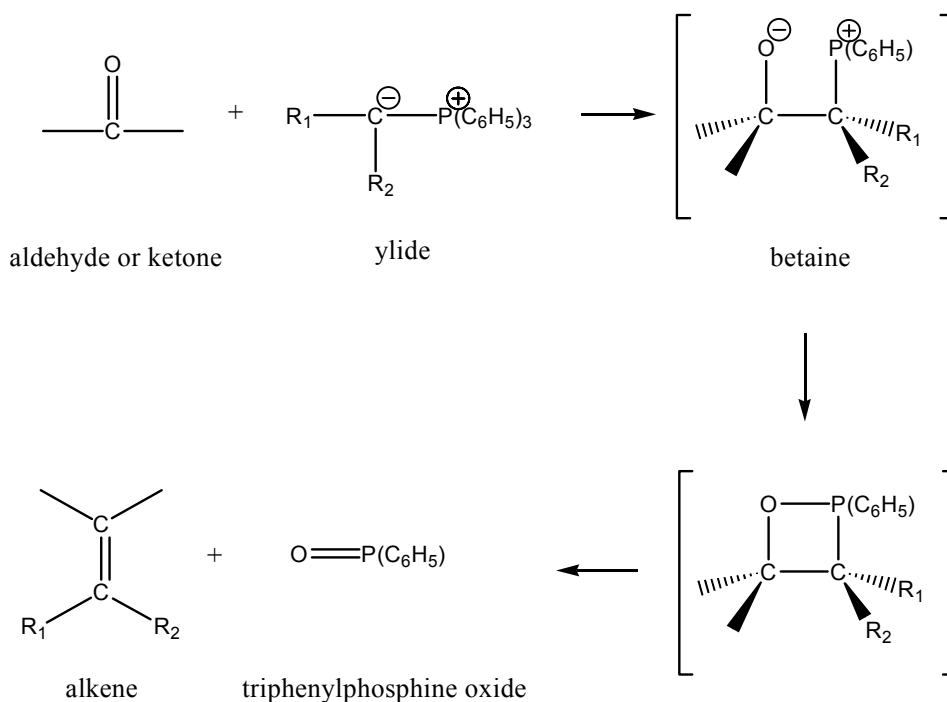


Figure 3.4 The Wittig reaction.

3.3.1.1 Procedure

In the first step of the reaction, the phosphonium salt was prepared by the reaction of triphenylphosphine with an organic halide, allyl chloride. The reaction is shown in Figure 3.5. 100 g of triphenylphosphine was added to an excess of allyl chloride and the solution was refluxed for 24 hours. The resulting slurry was cooled and the solid salt was collected by vacuum filtration. The salt was then washed with benzene and dried in a vacuum oven. Typical yields of the salt were around 48%.

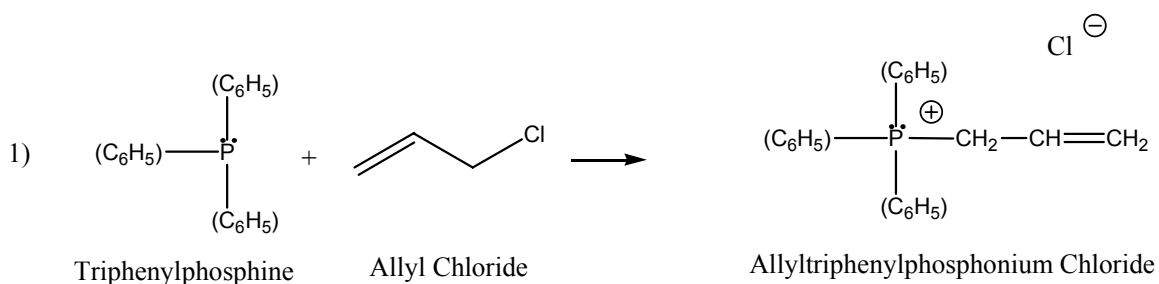


Figure 3.5 Salt formation for the Wittig Reacton

In the second step, the ylide is generated by reaction of the salt with a 1.5 molar quantity of butyllithium, then with a 2 molar quantity of butyraldehyde to generate the alkene. The reaction was done in a 500 mL kettle purged with argon and flamed to remove air and moisture. The allyltriphenylphosphonium chloride salt was dissolved in dry ether before adding butyllithium via a syringe through a rubber septum. A dark red solution resulted from adding the butyllithium, characteristic of the formation of ylide. The solution was then cooled in a dry ice/acetone bath prior to adding the butyraldehyde. Upon addition of the butyraldehyde, a creamy beige solution formed immediately. The reaction was allowed to proceed for several minutes at 10°C, and then decomposed with distilled water. The reaction sequence is shown in Figure 3.6.

The olefin was extracted from the water layer with ether, and the ether portions were combined. Most of the ether was then removed by rotary evaporation. A final work-up procedure was employed using petroleum ether to precipitate out most of the triphenylphosphine oxide from the product mixture. The olefin was then separated from solution by chromatography on a silica gel column using petroleum ether as the eluting solvent. Fractions were tested on TLC plates to determine the contents.

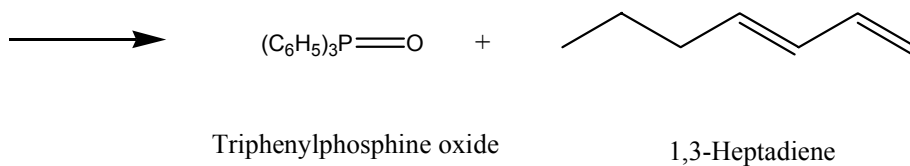
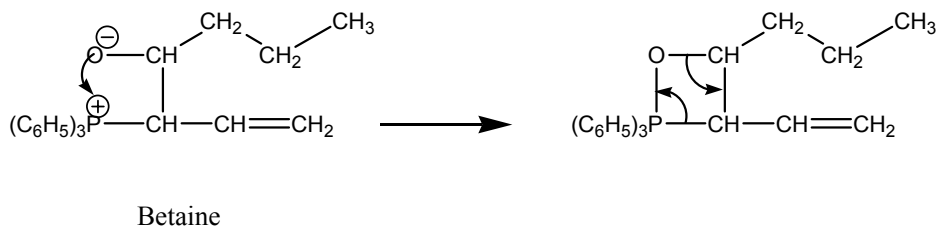
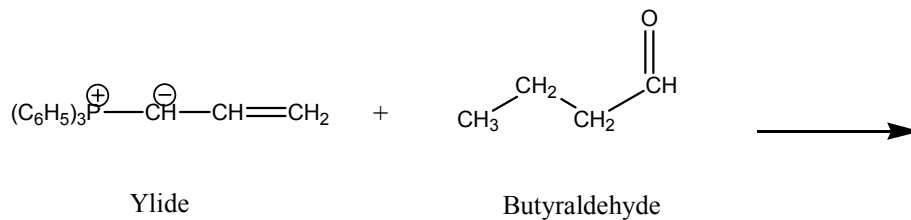
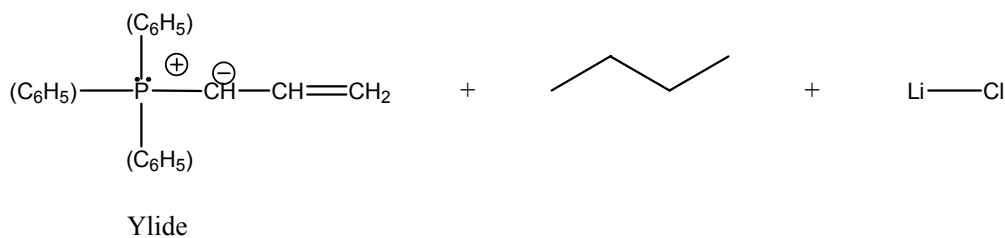
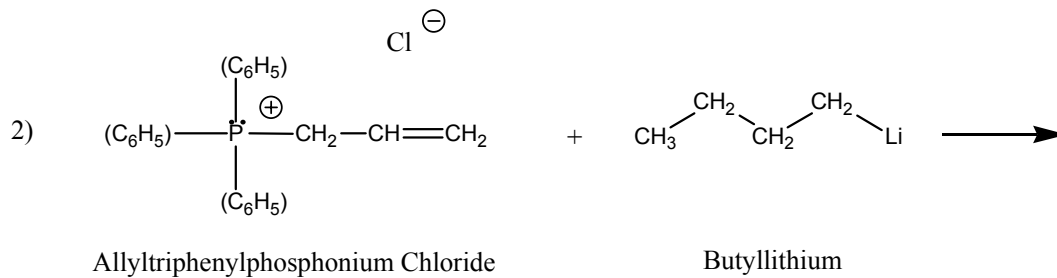


Figure 3.6 The Wittig reaction to form 1,3-heptadiene monomer

3.3.1.2 Results and discussion

Figure 3.7 shows the estimated NMR peaks for 1,3-heptadiene and the NMR spectrum of the synthesized monomer. The spectrum for the synthesized monomer shows peaks around 5 and 6 ppm, which can be correlated to those of the 1,3-diene protons. However, there are other peaks present which indicate that the monomer is impure. The presence of the other alkene hydrogen peaks could be a result of an isomer of 1,3-heptadiene, which was difficult to separate. In addition, there are some peaks at approximately 7 ppm which suggest the presence of another substance, possibly a by-product that contains an aromatic ring. The spectrum also shows the presence of the petroleum ether solvent, indicated by the large peaks around 1 and 1.5 ppm.

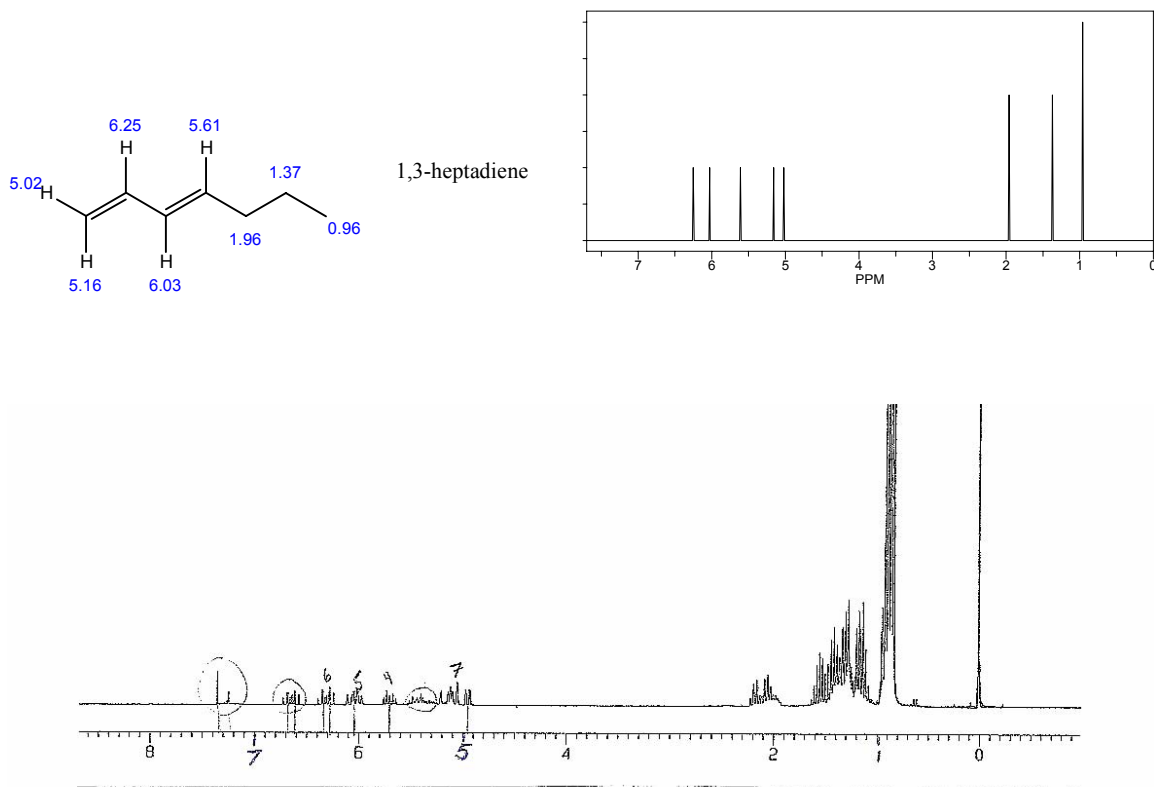


Figure 3.7 ^1H NMR spectrum of synthesized 1,3-heptadiene.

The diene was the first product eluted from the silica gel column, followed closely by another product, assumed to be the isomer. Due to the closeness in the rate of migration of the two products, it was difficult to separate the monomer product. Since a very small amount of monomer was obtained, the monomer portions that were collected contained some of this by-product.

3.3.2 Polymerization

3.3.2.1 Procedure

The collected heptadiene product was polymerized in a similar manner as the procedure for polymerizing 1,3-pentadiene. The same solvents, initiator, argon and SO₂ gases were used. The method differed slightly as described below.

The monomer portions collected from liquid chromatography were combined in a flask. Most of the petroleum ether was evaporated out, by heating the solution through the boiling range of 44-59° C to avoid any loss or reaction of the monomer due to heating. Approximately 15 mL of nitropropane was added to the solution, and weighed in a clean pre-baked 2-neck round bottom flask to be used in the polymerization. The flask was connected to the filled dry ice condenser, placed in a dry ice and acetone bath, and purged with argon for approximately 30 minutes while stirring. Then approximately 20 g of SO₂ was condensed into the flask, giving a large excess of SO₂ to monomer. A solution of approximately 1 mL of t-butyl peroxide was added to the solution via syringe through the septum and allowed to react for 1 hour. A tiny amount of white flakes dispersed in the solution appeared after some time. The solution was removed from the dry ice bath and allowed to warm to room temperature. Two liquid layers were visible while in the dry ice bath, and the top layer disappeared as the temperature warmed. This

indicated that the large excess of unreacted SO₂ was vaporized as the temperature warmed. Approximately 20 mL of nitromethane was added, and the white solid appeared to dissolve into solution. The white solid was then precipitated into 200 mL of methanol, and filtered out.

3.3.2.2 Results and discussion

Only trace amounts of product formed, therefore further analysis of the polymer was not attempted. The white product formed is insoluble in nitromethane alone. It is believed that the very low yield of polymer is due to impurities in the monomer. The presence of the by-product and/or petroleum ether in the solution may have interfered with the polymerization reaction, although the presence of petroleum ether in a subsequent reaction of SO₂ and 1,3 pentadiene did not prevent polymerization. It should also be noted that although the molar ratio of SO₂ to monomer is ideally 3:1, the copolymerization of SO₂ with heptadiene was done in a large excess of SO₂. Perhaps this large excess interfered with the radical polymerization of the monomer.

CHAPTER 4

CONCLUSIONS

Spectroscopy is a useful tool in understanding the occurrences in atoms and molecules during the radiation-induced degradation of polysulfones. XANES, or x-ray absorption near-edge structures spectroscopy, is especially useful for studying the transformations in the sulfur atom, which directly affect the sulfur-carbon bond involved in polymer degradation. XANES studies of the polysulfones exhibited a marked difference between those polymers with a C=C in the main chain backbone and those polymers lacking one. For example, irradiated polysulfones lacking a C=C in the backbone show the presence of a more reduced sulfur state resembling a sulfide group, while those containing a C=C in the backbone begin to show the presence of a more oxidized state of sulfur, such as a sulfonate or sulfate group. These results are consistent with previous XANES studies done on poly(butene sulfone), PBS, and poly(hexadiene sulfone), PHS.

Although the results from XANES do not give a clear picture of any mechanistic details of degradation, they do support the results obtained from in situ mass spectrometry during irradiation. The mass spectra of polysulfones lacking a C=C in the backbone indicate the generation of many volatile species upon irradiation, specifically SO₂, SO and small carbon chain fragments such as C₄, C₃ and C₂. The established decomposition pathway for poly(butene sulfone), PBS, results in the generation of 1-butene monomer and SO₂, followed by fragmentation of 1-butene into smaller fragment ions. Similar fragmentation patterns were observed in the mass spectrum of poly(2-

methyl pentene sulfone), P2MPS. The detection of C_5 and C_6 fragments also implicate the presence of monomer or other stable rearrangement of the monomer. In contrast, the mass spectra of the polysulfones containing a $C=C$ in the backbone show only the presence of SO_2 and SO . They do not show the presence of the smaller C_4 , C_3 or C_2 fragment ions. These results lead us to believe that radiation-induced degradation of these polymers results in the generation of a stable species which does not further fragment.

Poly(olefin sulfones) are synthesized via a radical polymerization mechanism, the reverse of the unzipping depolymerization caused by radiation. The radical polymerization is spontaneous and the reaction occurs rapidly in the presence of an initiator, which generates unstable highly reactive radical species. The polymerization of 1,3-pentadiene was successful, but that of 1,3-heptadiene was not. The reason for this is the impurity of the 1,3-heptadiene monomer. Therefore, an improved method for synthesizing the monomer is required to successfully complete the polymerization.

In conclusion, the work presented in this thesis suggests many future studies to be pursued. A thorough spectroscopic analysis of the polysulfones at different radiation doses should be completed. Another interesting pursuit would be to formulate a developer solution that will selectively dissolve the irradiated poly(hexadiene sulfone) and to subsequently analyze the dissolved polymer. An improved general synthesis of 1,3-dienes would facilitate the synthesis of a series of poly(unsaturated olefin sulfones).

REFERENCES

- 1) Thompson, L.F., Willson, C.G., Bowden, M.J. *Introduction to Microlithography*; John Wiley: New York, 1994.
- 2) Schnabel, W. *Polymer Degradation: Principles and Practical Applications* Macmillan Publishing Co., Inc: New York, 1981, 139, 131-135, 146-148, 95-98, 100, 133-137.
- 3) Davies, J. (1996). Synthesis of UV/X-ray Sensitive Polymers and their Applications as Resists, Ph.D. Dissertation, Louisiana State University.
- 4) Rabek, J.F. *Photodegradation of Polymers: Physical Characteristics and Applications*; Springer-Verlag: Berlin Heidelberg, 1996, 1-2
- 5) Reichmanis, E., O'Donnell, J.H. *The Effects of Radiation on High-Technology Polymers; ACS Symposium. Series 381*; American Chemical Society: Washington, 1989. 1-2, 5, 10
- 6) Reichmanis, E., MacDonald, S.A., Iwayanagi, T. *Polymers in Microlithography: Materials and Processes; ACS Symposium Series 412*; American Chemical Society: Washington, DC, 1989
- 7) Sinfelt, J.H., Meitzner, G.D. (1993) *Accounts of Chemical Research* **Vol. 26 #1**, 1-2
- 8) Koningsberger, Prins (1988). *Chemical Analysis* **Vol. 92**, 575, 577
- 9) Modrow, H., Calderon, G., Daly, W.H., de Souza, G.G.B., Tittsworth, R.C., Moelders, N., Schilling, P.J. (1998) *Journal of Synchrotron Radiation*
- 10) Wollersheim, O. et al. (1995) *Nuclear Instruments and Methods in Physics Research: Beam Interactions with Materials & Atoms* **B97**, 273-278
- 11) Sarret, G. et al (1999) *Geochima et Cosmchimica Acta* **Vol. 63**, 3767-3779
- 12) Atkins, P. *Physical Chemistry*, 5th Edition; W.H.Freeman and Company: New York, 1994
- 13) Munk, P. *Introduction to Macromolecular Science*; John Wiley & Sons: New York, 1989, 129
- 14) McMurray, J. *Organic Chemistry*; Brooks/Cole Publishing Co: Monterey, 1984, 710-711

15) J.D. Davies and W.H. Daly, U.S. Patent 5,922,518, issued July 13, 1999; J.D. Davies and W.H. Daly, U.S. Patent 6,103,866, issued Aug. 15, 2000

VITA

Gina Calderon obtained her Bachelor of Science degree in Microbiology at Louisiana State University in Baton Rouge, Louisiana in May of 1995. She then worked as a Research Associate in the X-ray Lithography group at the Center for Advanced Microstructures & Devices in Baton Rouge until she began her graduate studies in the Department of Chemistry at LSU. She is currently employed as a Senior Research Assistant in the Department of Biochemistry and Molecular Biology at the University of Texas M.D. Anderson Cancer Center in Houston, Texas. She is working on the x-ray crystallography of transcription proteins.